



Effect of non-uniform reactor cooling on fracture and constraint of a reactor pressure vessel

Journal:	<i>Fatigue & Fracture of Engineering Materials & Structures</i>
Manuscript ID	FFEMS-7296.R1
Manuscript Type:	Original Contribution
Date Submitted by the Author:	22-Jan-2018
Complete List of Authors:	Qian, Guian; Paul Scherrer Institute, Nuclear Energy and safety Niffenegger, Markus Sharabi, M. Lafferty, N.
Keywords:	reactor pressure vessel, Stress intensity factor, constraint effect, pressurized thermal shock, probabilistic fracture mechanics, Crack propagation



Highlights:

1. Fluid dynamics and fracture mechanics methods applied to integrity analysis of a RPV
2. Non-uniform cooling effect increases the crack tip constraint and K_I
3. Non-uniform cooling effects increases fracture frequency by 2 orders of magnitude
4. Probabilistic fracture mechanics method predicts a less conservative result

Review Copy

1
2
3
4
5
6
7
8
9 **Effect of non-uniform reactor cooling on fracture and constraint of**
10 **a reactor pressure vessel**
11

12
13 Guian Qian^{1,*}, Markus Niffenegger¹, Medhat Sharabi^{2,3}, Nathan Lafferty²
14
15

16 ^{1*}*Correspondent, Paul Scherrer Institute, Nuclear Energy and Safety Department, Laboratory*
17 *for Nuclear Materials, Villigen PSI, Switzerland, guian.qian@psi.ch*
18

19 ²*Paul Scherrer Institute, Nuclear Energy and Safety Department, Laboratory for Thermal*
20 *Hydraulics, Villigen PSI, Switzerland*
21

22 ³*Mansoura University, 35516 Mansoura, Egypt*
23
24
25
26
27
28
29
30
31
32
33
34
35
36
37
38
39
40
41
42
43
44
45
46
47
48
49
50
51
52
53
54
55
56
57
58
59
60

Effect of non-uniform reactor cooling on fracture and constraint of a reactor pressure vessel

Abstract

In the lifetime prediction and extension of a nuclear power plant, a reactor pressure vessel (RPV) has to demonstrate the exclusion of brittle fracture. This paper aims to apply fracture mechanics to analyze the non-uniform cooling effect in case of a loss-of-coolant accident (LOCA) on the RPV integrity.

A comprehensive framework coupling reactor system, fluid dynamics, fracture mechanics and probabilistic analyses for the RPVs integrity analysis is proposed. The safety margin of the allowed RT_{NDT} is increased by more than 16 °C if a probabilistic method is applied. Considering the non-uniform plume cooling effect increases K_I more than 30%, increases the failure frequency by more than one order of magnitude, and increases the crack tip constraint due to the ~~resulted~~ ~~resulting~~ higher stress. Thus, in order to be more realistic and not to be non-conservative, 3D CFD may be required to provide input for the fracture mechanics analysis of the RPV.

Keywords: reactor pressure vessel; stress intensity factor; constraint effect; pressurized thermal shock; probabilistic fracture mechanics; crack propagation

Nomenclature

a = crack depth, mm

b_0, b_1, b_2 and b_3 = coefficients for the polynomial approximation of stress

$F_\alpha(\mathbf{x})$ = crack-tip functions

$H(x)$ = Generalized Heaviside function

$h(x,a)$ = weight function for stress intensity factor

i_0, i_1, i_2 and i_3 = influence coefficients for the approximation of stress intensity factor

I = set of all nodes in the mesh

K_I = Mode I linear elastic stress intensity factor, $\text{MPa} \cdot \text{m}^{0.5}$

K_{Ic} = material fracture toughness, $\text{MPa} \cdot \text{m}^{0.5}$

K_{Ia} = crack arrest toughness, $\text{MPa} \cdot \text{m}^{0.5}$

M_m = free-surface correction for membrane stress

M_b = free-surface correction for bending stress

$N_i(\mathbf{x})$ = nodal shape function

P = fracture probability

1
2
3
4
5
6
7
8
9
10
11
12
13
14
15
16
17
18
19
20
21
22
23
24
25
26
27
28
29
30
31
32
33
34
35
36
37
38
39
40
41
42
43
44
45
46
47
48
49
50
51
52
53
54
55
56
57
58
59
60

$P(F | E)_i$ = conditional failure probability of vessel due to the i^{th} transient

Q = crack shape correction factor for stress intensity factor calculation

RT_{NDT} = nil-ductility transition reference temperature, °C

t_i = transient time, minute

T = temperature, °C

T -stress = second term of William's solution, MPa

u_i = standard DOFs of node i

σ = stress, MPa

σ_m = membrane stress, MPa

σ_b = bending stress, MPa

$\phi(E)_i$ = occurrence frequency of the transient

CFD = computational fluid dynamics

DOF = degree of freedom

ECC = emergency core cooling

FEM = finite element method

HTC = heat transfer coefficient

LBLOCA = large break loss-of-coolant accident

MBLOCA = medium break loss-of-coolant accident

MC = Monte Carlo

PTS = pressurized thermal shock

RCP = reactor coolant pumps

RPV = reactor pressure vessel

SIF = stress intensity factor

SIP = safety injection pumps

SBLOCA = small break loss-of-coolant accident

TWCF = through-wall cracking frequency

WPS = warm prestressing

XFEM = extended finite element method

1. Introduction

The reactor pressure vessel (RPV) in a nuclear power plant is not replaceable and thus its integrity determines the lifetime of the nuclear power plant. During the operation of the plant, the integrity of RPV should be assured, and the brittle failure of the RPV should be excluded [1-22]. A critical loading for a RPV is pressurized thermal shock (PTS), i.e. rapid cooling of sections of the hot and still pressurized RPV by injection of cold emergency coolant, which is ~~the resulted by-of~~ the loss-of-coolant accidents [1-3]. During a PTS, thermal gradients are leading to high stress in the RPV wall. On the other hand, the RPV material ages with neutron embrittlement and is susceptible to brittle fracture. Brittle fracture initiated by postulated or existing cracks may occur under PTS loading and this is generally considered to be the major threat to RPV integrity. Thus, the PTS analyses has to be performed and updated during operation according to the crack driving force and aged material property. The physical model for the integrity analysis of a RPV is shown in Fig. 1a. The assessment results can be used in the frame of the lifetime prediction and license renewal of a plant.

The integrity analysis of the RPV is generally conducted according to fracture mechanics methods. In a deterministic way, as applied in European countries [3], the analysis is performed for a fixed crack and material property. In the analysis, the stress intensity factors (SIFs) K_I of postulated cracks are compared with fracture toughness K_{Ic} . A component is regarded as safe if the calculated SIF is lower than K_{Ic} . In contrast, probabilistic assessment [3, 8, 9] considers distribution functions of crack parameters and material properties and provides a more rational result with consideration of uncertainties. In the probabilistic analysis the ~~concerning-relevant~~ parameters are considered as random following a certain distribution function. In a Monte Carlo (MC) calculation the random parameters are varied and thousands of deterministic analyses are performed. The probability for a component failure is simply the ratio between the ~~failure-resultscases resulting in failure~~ and the total number of calculations. The flowchart of a probabilistic analysis is shown in Fig. 1b.

A comprehensive integrity analysis includes the reactor system analysis, fluid dynamics analysis, structural mechanics analysis, fracture mechanics and probabilistic analyses, as shown in Fig 1c. Firstly, the accident scenario is simulated with a nuclear system code like RELAP5 [23] in order to obtain the pressure and temperatures distributions in the RPV for the whole transient. However, RELAP5 assumes axisymmetric temperature distribution and neglects non-uniform cooling caused by cooling plumes due to the mixing of hot and cold water. In order to consider this non-uniform cooling effect, 3D computational fluid dynamics (CFD) simulations are performed [24], which provides temperature distribution for the fracture mechanics calculations. Besides the 3D CFD calculations, an analytical method to consider the local effect of cooling plumes is achieved by the code GRS-MIX [26], which uses an empirical model to calculate the local heat transfer

1
2
3
4
5
6
7
8
9 coefficients (HTC) and water temperatures. Both structural and fracture mechanics analyses are performed with
10 the finite element method (FEM). However, if the loading conditions and geometry are simplified as one-
11 dimensional, fracture mechanics analysis can be performed by FAVOR [6], which is based on analytical
12 formulas for the calculation of SIFs of cracks in axi-symmetrically loaded cylinders. This code is also a
13 probabilistic tool that calculates crack initiation and failure probabilities based on the MC simulations. The
14 parameters transfer between the numerical models is shown in Fig. 1c. It should be pointed out that RELAP5
15 only provides axisymmetric results, whereas CFD and GRS-MIX consider this non-uniform effect.

16
17 Due to the significance and nuclear safety, a lot of work has been done concerning the safety assessment of
18 RPVs under accident scenarios [1-22]. Both deterministic and probabilistic integrity analysis of a RPV
19 subjected to PTS transients considering uniform RPV cooling have been performed by linear elastic (LEFM)
20 and elastic-plastic fracture mechanics (EPFM) [1-5, 13, 16-22]. A review of the procedures, methods and
21 computer codes for the RPV integrity assessment is given in [18]. Probabilistic assessment is performed for a
22 RPV subjected to small break loss-of-coolant accident (SBLOCA) and medium break loss-of-coolant accident
23 (MBLOCA) transients [19, 22]. A plastic correction factor has been introduced for the underclad crack in the
24 PTS calculations [14]. Applying the material toughness obtained from small specimen to the large RPV has
25 been an important topic. The constraint effect of a shallow crack tip on the fracture toughness during a transient
26 has been analyzed in [2, 10, 12]. González-Albuixech et al. [21] used extended finite element method (XFEM)
27 for the fracture mechanics calculation of the RPV containing different types of cracks. The advantage of XFEM
28 in modeling a crack in complicated structure is demonstrated. Recently, research work has been given on the
29 effect of PTS-loadings caused by the nonuniform temperature distribution due to cold water plumes. Some
30 engineering codes, e.g. KWU-MIX, REMIX and GRS-MIX, have been developed based on analytical methods
31 to determine the thermal-hydraulic process of the emergency cooling water from the injection location to the
32 position in the downcomer [3, 23-25].

33
34 This paper aims to apply fracture mechanics method for a comprehensive assessment of a RPV. A probabilistic
35 analysis is performed and the non-uniform cooling effect in the RPV is analyzed. The PTS transients are
36 analyzed with RELAP5 [23], GRS-MIX [26] and CFD methods [24]. SIF of the postulated cracks and T-stress
37 are calculated to quantify the crack driving force and the constraints of the crack tip. Based on the calculations,
38 the safety margin of the RPV is calculated in terms of RT_{NDT} , the nil-ductility transition temperature. The first
39 part of this paper is an introduction, followed by the transient calculation by RELAP5, GRS-MIX and CFD. The
40 third part is structural mechanics and fracture mechanics analyses. The fourth part is deterministic and

1
2
3
4
5
6
7
8
9
10 probabilistic fracture mechanics analyses. The fifth and sixth parts are the safety margin definition of maximum
11 RT_{NDT} according to deterministic and probabilistic methods.

12 **2. PTS loading transient calculations**

13 **2.1 Transients calculations by RELAP 5**

14 A RELAP5 [23] model, developed at Paul Scherrer Institute to simulate loss of coolant accidents for a reference
15 two-loop pressurized water reactor (PWR), was used assuming a break in the hot leg piping. The emergency
16 core cooling system (ECCS) includes high pressure injection pumps capable of injecting cold water into both
17 cold legs and, in addition, two accumulators, one per cold leg which are actuated when the pressure decreases to
18 intermediate values.
19

20
21 Break sizes of 3, 70 and 450cm² in the hot leg are simulated. The three transients correspond to SBLOCA,
22 MBLOCA and large break loss-of-coolant accident (LBLOCA) transients. The output from the RELAP5
23 calculations, i.e. the fluid temperatures at the RPV core, fluid pressures and the HTC between the coolant and
24 the RPV wall, are used as initial and boundary conditions input for the GRS-MIX, CFD calculations, and for the
25 structural and fracture mechanics calculations. The transients calculated by RELAP 5 are shown in Figs. 2a, 2b
26 and 2c.
27
28

29 **2.2 Transients calculations by GRS-MIX**

30 RELAP5 and other similar system codes can predict integral behavior of the reactor during transients and give
31 predictions of relevant variables fairly well without the need of high computational resources. Nevertheless,
32 these methods fail to predict local effects and three-dimensional phenomena such as those taking place during
33 PTS. It is therefore needed to adopt other methods that are more accurate and also computationally efficient.
34 Within this framework, GRS-MIX is used which is a software developed by GRS (Gesellschaft für Anlagen-
35 und Reaktorsicherheit). The code has a number of implemented engineering correlations and the relevant
36 correlations can be used based on the estimated flow regime. The output of the code gives the temperatures and
37 heat transfer coefficients at the prescribed positions downstream in the downcomer.
38
39
40

41 The dedicated engineering code GRS-MIX [26] is used in order to study ~~the~~ break sizes ~~that ranging~~ from
42 small to large break LOCAs which is not feasible with CFD due the large computational resources needed to
43 conduct these simulations. The engineering correlations implemented in this GRS-MIX were developed based
44 on the experimental data obtained from the UPTF test facility [26]. The Froude number is used to specify the
45 flow conditions in the cold leg which can be either stratified or counter-current flow. A modified Dittus-Boelter
46 equation based on the UPTF data is adopted to calculate the heat transfer coefficient using the plume
47 parameters. The velocity inside the plume is calculated from the Chen and Chen correlation [27]. The input data
48
49
50

needed for GRS-MIX such as cold water injection mass flow rate, the temperature of the back flow in the cold and the temperature outside the plume are all obtained using approximation of RELAP5 results. For the heat transfer coefficient outside the plume, the experimental data showed that, it can be approximated with a constant value of $1500 \text{ W/m}^2 \cdot \text{K}$ independent of the injection flow rate.

The results of the coolant temperature and the heat transfer coefficient for different break sizes using GRS-MIX are shown in Figs. 2d and e. By comparing with the results from RELAP5 in Figs. 2a and b, it can be observed that the water temperature is significantly colder and the HTC changes substantially inside the plume. It should be considered that data obtained for the PTS analyses using GRS-MIX are subjected to several sources of uncertainties due to difference in the geometry between the UPTF test facility and the RPV adopted in the current study. In addition, the input data for GRS-MIX is based on temperatures from RELAP5 which is one-dimensional and averaging approximations were adopted. This proves that CFD calculations, though time-consuming, ~~but they are~~ necessary to fairly represent the details of the mixing phenomena and cooling in the downcomer. Also, different thermal-hydraulic conditions like asymmetric cold water injections and injection of cold water at two different locations in the same cold leg contribute to uncertainties regarding validity of GRS-MIX correlations when applied to different problem configurations than those developed for.

2.3 Transients calculations by CFD

ANSYS FLUENT 16.0 is used in the analyses made using CFD methods in order to predict the three-dimensional behavior of the flow in the cold leg and plume oscillation in the downcomer. The best practice guidelines for application of CFD in nuclear safety [24] are followed in the present analyses. All relevant geometrical details of the RPV are considered in the CFD model including: injection pipes, inlet nozzles and curvatures and the neutron shield located in the downcomer which have strong impact on the flow development in the downcomer. In order to study mesh sensitivity of the results, two meshes were constructed using fully structured mesh topology with 3.3 and 5.1 million nodes. Special attention was taken to have more refinement in locations of the plumes and cold legs where injection of cold water is expected. No significant differences of the plume behavior or temperature distributions were noticed for the case of higher mass flow rate injection of cold water. All the simulations in the current study were conducted making use of the finer mesh shown in Figs. 3a and b. Further details about mesh strategy adopted in the present study can be found in [28]. A fully structured mesh of 5.1 million nodes is created as shown in Figs. 3a and b and the mesh sensitivity study showed insignificant change in the results when the simulations were repeated with different meshes. The SST $k-\omega$ model is used to model the turbulence and the y^+ for the first node beside the wall is around 100. Second order discretization schemes are adopted for the convection and transient terms in the governing equation.

1
2
3
4
5
6
7
8
9
10 The initial and boundary conditions are obtained from the accident analyses made using RELAP5 for two break
11 scenarios in the hot leg; an SBLOCA of 3 cm² and a MBLOCA of 70 cm². For the SBLOCA, the high pressure
12 Safety Injection Pumps (SIP) inject emergency cooling water of 12 kg/s and temperature of 30 °C in each of the
13 cold leg, while the pressure remains at a high value of 9.8 MPa after an initial decrease following the break. On
14 the other hand, for the MBLOCA, following the initiation of SIP injection, the accumulators inject cold water of
15 200 kg/s and 10°C. ~~A-s~~Simulation times of 2500 s and 800 s were ~~performed-used~~ for the SBLOCA and
16 MBLOCA scenarios, respectively. Figs. 3c and d show contours of temperature on the RPV walls at two
17 different instants for the two scenarios. The results show the temperature stratification at the inlet nozzles, ~~This~~
18 is especially evident for the SBLOCA case the thermal stratification prevails in cold leg due to the lower
19 injection mass flow ~~rate-rate~~; however, the temperature gradients for the MBLOCA case are larger. The figures
20 also confirm the highly three-dimensional behavior of the plume cooling in the downcomer and the importance
21 of the detailed CFD simulation to precisely capture these phenomena.
22

23 3. Structural mechanics and fracture mechanics analyses validation

24 Based on the output of RELAP5 and GRS-MIX, the thermal and fracture mechanics analysis is
25 performed by FAVOR, whereas the thermal mechanical analysis based on CFD results is performed using the
26 FEM by ABAQUS v 6.14 [2829]. RELAP5 and GRS-MIX outputs are one-dimensional, meaning that the
27 calculated coolant temperature, pressure and heat transfer coefficient are uniform in the inner vessel wall and
28 they only vary with the transient time. However, the output with 3D CFD models is non-uniform in the vessel
29 wall. In the FAVOR code, it is assumed that the coolant is uniform in the inner vessel wall and FAVOR is thus
30 not able to capture the non-uniform cooling effect. 3D XFEM is resorted to analyze the non-uniform cooling
31 effect on K_I .
32

33 The beltline region, which is the most irradiated part of the RPV, is modeled by the 3D FEM. The inner side of
34 the RPV is assumed to be subjected to a thermal shock caused by the falling plume of emergency cooling water.
35 The time dependent 3D temperature distribution in the RPV calculated in the preceding CFD simulation, which
36 defines the cooling effect and the thermal loads, is interpolated onto the finite element mesh. The finite element
37 mesh is built using quadratic hexahedron elements to facilitate the interpolation of temperatures taken from the
38 CFD mesh. Figs. 3c-3f show the temperature and stress distributions of the vessel during the SBLOCA and
39 MBLOCA. Material mechanical properties are described in [1, 2, 18-22]. About 800 seconds of the MBLOCA
40 and 2500 seconds of SBLOCA transients are calculated, which correspond to the most relevant time for PTS
41 analysis. The results of the mechanical model are used as input for the fracture mechanics analysis in the next
42
43
44
45
46
47
48
49
50

part; furthermore a probabilistic assessment will be performed based on the structural and fracture mechanics analyses.

In LEFM analysis, K_I is calculated. Two methods are used in this paper for K_I computation: ~~ie~~ the weight function method (influence function method) implemented in the FAVOR code and the interaction integral (domain integral) implemented in the FEM (or XFEM) frameworks. The weight function procedure developed by Bückner [2930] is an analytical method for the determination of SIFs based on FEM. If the weight function is known for a crack in a component, the SIF can be obtained by multiplying this function by the stress distribution and integrating it along the crack length.

In the FAVOR code [6], SIF is calculated by the influence function method, as listed in Eqs. (1) and (2). The SIF of surface cracks is written as

$$K_I = \sqrt{\frac{\pi a}{Q}} [b_0 i_0 + b_1 i_1 a + b_2 i_2 a^2 + b_3 i_3 a^3]. \quad (1)$$

The coefficients i_0 , i_1 , i_2 , i_3 , are calibrated by the FEM. b_0 , b_1 , b_2 and b_3 are coefficients for the polynomial approximation of stress, a is the crack depth, Q is the crack shape correction factor.

For an embedded crack, stress distribution is based on the resolution of nonlinear applied stresses through the RPV wall thickness into the linear superposition of approximate membrane and bending stress components. K_I is expressed as

$$K_I = \sqrt{\frac{\pi a}{Q}} (M_m \sigma_m + M_b \sigma_b). \quad (2)$$

M_m is free-surface correction for membrane stress, M_b is free-surface correction for bending stress, σ_m is membrane stress, and σ_b is bending stress.

In FEM, the SIF is normally calculated by interaction integral or domain integral which is implemented in the commercial software Abaqus. The modeling of a 3D crack in FEM, as shown in Fig. 4a, takes many efforts. The XFEM, which enriches the finite element ~~approach~~ approximation space with special functions that are able to describe the discontinuity and introduce the singular behavior of the crack front, makes the modeling of the crack easier and the results ~~somehow~~ more independent of the mesh [3031]. In XFEM, the displacement field is approximated by:

$$\mathbf{u}_{XFEM}(\mathbf{x}) = \sum_{i \in I} N_i(\mathbf{x}) \mathbf{u}_i + \sum_{i \in J} N_i(\mathbf{x}) H(\mathbf{x}) \mathbf{a}_i + \sum_{i \in K} \left[N_i(\mathbf{x}) \sum_{\alpha=1}^4 F_{\alpha}(\mathbf{x}) \mathbf{b}_{i\alpha} \right], \quad (3)$$

where I is the set of all nodes in the mesh, $N_i(\mathbf{x})$ are the classical shape function and \mathbf{u}_i are the standard DOFs of node i (\mathbf{u}_i represents the physical nodal displacement for non-enriched nodes only). The subsets J and K contain

the nodes enriched with the Generalized Heaviside function $H(x)$ or the crack-tip functions $F_a(x)$, respectively, and \mathbf{a}_i , \mathbf{b}_{ia} are the corresponding DOFs. Mesh details of an axial surface crack in the ring and nozzle regions ~~with-represented using~~ XFEM are shown in Figs. 4b and 4c.

Material fracture toughness is based on ~~different~~ databases for the RPV steels, e.g. ASME method [3432], FAVOR model, Master Curve method [3233], etc. According to ASME [3432], the fracture toughness is calculated by

$$K_{IC} = 36.5 + 22.78 \exp[0.036(T - RT_{NDT})] \quad (4)$$

The neutron irradiation effect is considered in RT_{NDT} .

As part of the quality assurance, the SIF calculated by FAVOR, FEM, XFEM are compared for a surface crack subjected to MBLOCA, as shown in Fig. 5a. An axial semi-elliptical crack, which has the depth of 17 mm and aspect ratio (length/depth) of 6 is postulated in the deterministic analysis. The crack geometry is according to German KTA rule, which is consistent with the two times nondestructive examination limit. The variation of SIF with temperature is due to the thermal gradient formed in the vessel wall and the variation of pressure history with transient time. A general agreement is achieved among the used methods. The meshes and modeling for FEM and XFEM are shown in Figs. 4a, 4b and 4c. The results calculated from FAVOR, FEM and XFEM are in reasonable agreement.

4. Deterministic and probabilistic fracture mechanics analyses

4.1 Deterministic fracture mechanics analysis

4.1.1 K_I calculations

The temperature of MBLOCA and SBLOCA transient with and without considering non-uniform cooling calculated by CFD, GRS-MIX and RELAP5 are compared in Fig. 5b and 5c. Obviously the vessel wall temperature within the plume region is lower than that outside, especially for MBLOCA. The CFD calculation (Fig. 5c) shows that in case of a SBLOCA, almost no difference between temperatures in and outside the cooling plume region exists, which is a consequence of the better mixing of cold and hot water in the downcomer. This is because the much lower injection mass flow rate in this case results in flow dispersion at the blockage formed by the neutron shield and does not allow for the development of a prominent cold plume as in the MBLOCA case. The temperature profile in the cooling plume is used to calculate SIF of the assumed cracks. The original FAVOR code is modified to allow reading of the RPV temperature distribution calculated by CFD. This change of FAVOR is applicable for both deterministic and probabilistic analyses. FAVOR was

1
2
3
4
5
6
7
8
9
10 modified to compute the mechanical response with a given prescribed through-wall temperature distribution
11 from the 3D CFD calculation. The given through-wall temperature is taken from either within or outside of the
12 plume in the 3D RPV model. Since FAVOR is a probabilistic code, the modified FAVOR is also used to perform
13 probabilistic fracture mechanics analysis with the 3D CFD output.

14
15 In the deterministic assessment, an axial surface crack with depth of 17 mm and aspect ratio (length/depth) of 6
16 is considered. It is worth mentioning that 17 mm equals to 1/10 of the vessel wall thickness and corresponds to
17 2 times the nondestructive detection limit. The integrity analysis of the RPV, subjected to SBLOCA, MBLOCA
18 and LBLOCA (Figs. 2 and 3), are studied with deterministic method. The comparison of K_I with K_{Ic} ($RT_{NDT}=93$
19 °C, limiting value given by RG 1.99 Rev. 2) is shown in Figs. 6a and 6b. It is seen that for most of the transients
20 K_{Ic} is higher than K_I , meaning that no crack initiation will occur. However, during the MBLOCA transient, K_I is
21 higher than K_{Ic} for a large part of the time. Compared to the case without considering plume cooling, K_I based
22 on the transients calculated by GRS-MIX is increased significantly by considering plume cooling effects. This
23 is due to the much colder water temperature and higher HTC inside the plume. If temperatures are based on
24 CFD calculations, the peak of K_I of the cracks inside the plume increases more than 40% compared with that
25 averaged (outside). The peak K_I of the crack in the plume is increased more than 30% compared to that outside
26 the plume.
27
28
29

30 Thus, neglecting the non-uniform cooling effect in the safety assessment is a non-conservative simplification.

31
32 In addition, it should be noted that RELAP5, GRS-MIX and CFD are three codes that adopt completely
33 different approaches to simulate the heating and mixing process of the injected cold water. RELAP5 is a best
34 estimate one-dimensional coarse-grid simulation code that is not capable to take into consideration the plume
35 cooling or thermal stratification, though it can provide the boundary conditions for other methods based on the
36 integral analyses of the transient. On the other hand, GRS-MIX is based on a number of engineering
37 correlations developed from UPTF-TRAM experiments for pressurized water reactors. Different flow regimes
38 can be distinguished and heating of the injected water can be determined at different downstream positions in
39 the downcomer. Though, due to geometrics differences of the adopted design in the present study and
40 differences in conditions (e.g., asymmetric injections), there is uncertainty in its predictions. CFD instead
41 consider the exact details of geometry and boundary conditions. Best practice guidelines were followed for
42 meshing and model selections.

43
44
45
46 From the above, the authors believe that the differences are greatly attributed to the different approaches (and
47 the validity of each method, especially for GRS-MIX when it is applied to different geometry and different
48 injection configurations) adopted in each code and CFD results are the most realistic ones and there is no error
49

transfer in steps of calculations. Though, CFD can be used only for selected cases due to computational expenses, and a full analyses of PTS still need to rely on other less detailed methods (such as engineering models or system codes) but also take into consideration the uncertainty in the prediction as demonstrated in this paper.

4.1.2 T-stress calculations

The elastic T-stress, or the second term of the Williams series expansion for linear elastic crack-tip fields, calculated by the interaction integral implemented in Abaqus 6.14, is used to analyze the crack tip constraint [3334-3637]. As shown in Figs. 6c and 6d, T-stress generally decreases with the transient time and then increases. This trend is opposite to that of SIF shown in Figs. 6a and 6b. At the initial state, the stress is mainly caused by the high internal pressure and is relatively high. With increasing thermal stress and decreasing of internal pressure, the level of stress triaxiality of the RPV is significantly decreased. And The T-stress decreases until achieving its minimum value. With the repressurization and increase of SIF, T-stress increases as the pressure increases the stress triaxiality. It is also seen in Figs. 6c and 6d that the non-uniform cooling effect increases the T-stress value due to the increasing of the stress in both axial and circumferential directions.

During the SBLOCA, T-stress displays a similar trend as that during MBLOCA transient. The difference is that T-stress variate-varies more significantly for the MBLOCA due to the higher thermal gradient. The negative T-stress means constraint loss occurs, which implies that the application of K_{Ic} based on plane strain specimens to the RPV leads to a conservative result. In order to get a more precise result, the fracture toughness from the test standards should be adjusted to the real component by considering the constraint.

4.2 Probabilistic fracture mechanics analysis

In the probabilistic analysis, the randomness of K_{Ic} is based on a Weibull distribution and the probability for crack initiation at a certain K_I is

$$P(K_{Ic} \leq K_I) = \begin{cases} 0 & K_I \leq a_K \\ 1 - \exp\left\{-\left[\frac{K_I - a_K}{b_K}\right]^{c_K}\right\} & K_I > a_K \end{cases}, \quad (5)$$

where

$$a_K = 21.27 + 9.18 \exp[0.041(T - RT_{NDT})], \quad (6)$$

$$b_K = 17.16 + 55.10 \exp[0.014(T - RT_{NDT})], \quad (7)$$

$$c_K = 4. \quad (8)$$

K_{Ia} model is developed based on a lognormal distribution ~~of-fitted to data from an~~ ORNL database [6]. The median of K_{Ia} model is written as

$$K_{Ia} = 30.00 + 77.70 \exp[0.016(T - RT_{NDT})] \quad (9)$$

The probabilistic analysis is performed for the beltline region of the vessel, which includes two rings and a welding region which are exposed to high neutron irradiation. In the probabilistic analysis, the crack density, depth, location, orientation, aspect ratio, ΔRT_{NDT} , K_{Ic} and K_{Ia} are assumed to be random variables [11]. The mean depths of surface and embedded cracks are 5 mm and 1.85, 6.29 or 4.03, 8.92 mm (depending on ring or welding, small or large cracks), respectively. The crack distributions of the surface and embedded cracks in this study are shown in Fig. 7a. It should be noted that for the deterministic analyses, only a fixed crack is considered. A large population of cracks is considered for the probabilistic analysis. The distributions of cracks, density, depth, aspect ratio are described in the manuscript. FAVOR is used for probabilistic fracture mechanics analysis based on the output of RELAP5, GRS-MIX and 3D CFD calculations. The FAVOR code is modified to compute the mechanical response and perform probabilistic analysis with a given prescribed through-wall temperature distribution taken from 3D CFD analysis. The results from XFEM models are used only in deterministic analysis to compare and validate the stress intensities.

The calculated crack initiation and failure probabilities for the three transients are shown in Fig. 7b. The conditional failure probabilities are used to calculate the cumulative failure frequency, which will be discussed later. It is seen that the probabilities based on GRS-MIX output ~~is-are~~ higher than those based on the RELAP 5 output. This means the probabilities increase if plume cooling effects are considered. For MBLOCA it is shown that the probabilities inside the plume are more than 9 orders of magnitude higher than that outside the plume which is in agreement with the K_I analysis. This is because the much lower temperature in the non-uniform cooling region occurs and thus increases the K_I and failure probabilities.

5. Determination of maximum RT_{NDT} according to deterministic method

In the deterministic analysis, the limiting K_{Ic} -temperature curve and the maximum allowed RT_{NDT} should be calculated to guarantee the safety of the irradiated RPV during the operation and used in the framework of lifetime extension. The maximum allowed RT_{NDT} are determined by maximum or tangent criteria for the postulated transient and crack geometry. This ~~is computed by shifting the indicates that the~~ K_{Ic} -temperature curve ~~is-shifted~~ until it is ~~interecepted-intersected~~ to their peak value if warm prestressing (WPS)-effects are considered or tangent to the calculated K_I -temperature curve of the transient under investigation. If the K_{Ic} -temperature curve is tangent to the K_I -temperature curve, K_{Ic} is always higher than K_I during the whole transient and thus no crack initiation occurs. WPS effect means that no crack initiation will occur if the material has been

Formatted: Font: Italic

Formatted: Subscript

1
2
3
4
5
6
7
8
9
10 prestressed at a higher temperature before reloaded above the K_{Ic} curve at a lower temperature. In the safety
11 margin analysis, the maximum criteria can be used if the WPS effect is considered. For the same K_I -
12 temperature curve, the maximum criteria predicts a larger safety margin and thus decreases the conservatism of
13 the results. According to both tangent and maximum criterion, the maximum allowed RT_{NDT} of the irradiated
14 RPV is determined. This determines the maximum allowed RT_{NDT} of the irradiated RPV. In this part, the
15 maximum allowed RT_{NDT} values according to maximum and tangent criteria for the axial surface crack with a
16 depth of 17 mm and aspect ratio of 6 are evaluated, as shown in Fig. 8. The most critical transient, i.e.
17 MBLOCA transients calculated from RELAP5, GRS-MIX and 3D CFD are used and the axial surface cracks
18 are postulated in the cylinder ring and nozzle regions. According to the maximum criteria, the maximum
19 allowed RT_{NDT} is 56.9 °C for the crack in the nozzle region based on CFD output, and 90.2 °C, 115.7 °C and
20 136.2 °C for the cracks in the ring region based on the CFD, GRS-MIX and RELAP5 output. According to the
21 tangent criteria which do not consider WPS-effects, the maximum allowed RT_{NDT} is 36 °C for the crack in the
22 nozzle region based on CFD transient, and 68.5 °C, 81 °C and 104 °C for the cracks in the ring region based on
23 the CFD, GRS-MIX and RELAP5 output. The CFD output leads to the lowest allowed RT_{NDT} values. This
24 means that these results may not be conservative without considering the non-uniform cooling effects with CFD
25 calculations. Maximum allowed RT_{NDT} values are used to limit the lifetime of the RPV.

30 6. Safety margin according to probabilistic fracture mechanics method

31 6.1 Cumulative failure frequency

32 The conditional failure probabilities are calculated based on the RELAP5, GRS-MIX and CFD calculated
33 temperatures. In the following, the conditional probabilities due to the SBLOCA, MBLOCA and LBLOCA are
34 used to calculate the cumulative failure frequency, which can be directly used as safety assessment of the RPV.
35 The total cumulative failure frequency $\phi(F)$ under several transients is determined from the summation of the
36 products of the individual transient occurrence frequency and the conditional failure probability, as

$$37 \phi(F) = \sum_i \phi(E)_i P(F|E)_i, \quad (10)$$

38 where $\phi(E)_i$ is the occurrence frequency of the i^{th} transient, $P(F|E)_i$ is the conditional failure probability of
39 vessel due to the i^{th} transient. F denotes the failure caused by event E. The occurrence frequencies for the
40 SBLOCA (3 cm²), MBLOCA (70 cm²) and LBLOCA (450 cm²) are 4.62×10^{-3} /year, 4.52×10^{-4} /year and
41 3.30×10^{-6} /year, respectively [18, 19].

42 The cumulative failure frequencies are calculated and listed in Table 1. The cumulative failure frequency based
43 on the RELAP5 input is 2.54×10^{-9} /year. Based on GRS-MIX, the frequency is 2.98×10^{-8} , which is one order
44

Formatted: Font: Italic

Formatted: Subscript

higher than that based on RELAP5. This is because the GRS-MIX data considered the non-uniform cooling effect whereas the RELAP5 data is from outside the plume. The cumulative failure frequency considering the non-uniform cooling based on CFD transients is 2.07×10^{-7} /year, which is higher than those based on RELAP5 and GRS-MIX data. This is in agreement with the deterministic analysis shown in Fig. 6. It is also shown in Table 1 that considering plume cooling effects increases the total failure frequency by 1-2 orders of magnitude. Nevertheless, all the failure frequencies fulfill the acceptance criterion (less than 1×10^{-6} through-wall cracks per year) for RPVs [9]. Therefore, the RPV is regarded as safe from probabilistic study, whereas the deterministic analyses predict crack initiation.

6.2 Maximum RT_{NDT} according to probabilistic fracture mechanics

In the USA, probabilistic methods are applied by US NRC to define the screening criteria [8, 9]. The NRC regulation [8] specifies limits of 132°C (270°F) and 149°C (300°F) on RT_{NDT} for the axially-oriented welds (as well as plates and forging) and circumferentially-oriented welds in the beltline region of the vessel. These limits on RT_{NDT} are limits according to an annual through-wall cracking frequency (TWCF) limit of 5×10^{-6} events/year. Since the early 1980s, several conservatisms have been quantified and a re-examination of the technical basis for these screening limit has been undertaken and risk-informed revision of the PTS rule and the screening limit have been developed. Recommendations on toughness-based screening criteria for PTS are provided in [8] based on RELAP and FAVOR calculation, the method is shown in Fig. 9a. According to the new screening criteria, the probabilistic screening criterion is defined as 1×10^{-6} events/year [9].

With the probabilistic results correlation between the maximum RT_{NDT} of the irradiated material and a failure frequency can be defined. According to the probabilistic results calculated for weld and forgings (ring material) shown in Fig. 9b, both failure frequency according to circumferential weld and forgings depending on the maximum RT_{NDT} show a similar trend. The tendencies for the circumferential weld and the forgings are determined by the Least-Square method, as shown in the following equations.

With the transients from RELAP5, TWCF for the ring and welding materials are calculated:

$$TWCF_{ring} = 9.91 \times 10^{-28.5} \times (RT_{NDT})^{10.03} / \text{year}, \quad (11)$$

$$TWCF_{weld} = 3.72 \times 10^{-33.08} \times (RT_{NDT})^{11.09} / \text{year}, \quad (12)$$

With the transients from GRS-MIX, TWCF for the ring and welding materials are:

$$TWCF_{ring} = 9.48 \times 10^{-26.31} \times (RT_{NDT})^{9.32} / \text{year}, \quad (13)$$

$$TWCF_{weld} = 2.49 \times 10^{-32.08} \times (RT_{NDT})^{11.10} / \text{year}, \quad (14)$$

With the transients from 3D CFD, TWCF for the ring and welding materials are:

$$TWCF_{ring} = 2.47 \times 10^{-25.90} \times (RT_{NDT})^{9.91} / \text{year}, \quad (15)$$

$$TWCF_{weld} = 1.90 \times 10^{-31.82} \times (RT_{NDT})^{11.84} / \text{year}, \quad (16)$$

Therefore, based on the PTS Screening Criteria it is also possible to determine the maximum RT_{NDT} . For a given allowable failure frequency of 1×10^{-6} an allowable RT_{NDT} for the circumferential weld and the forgings according to the above equations are calculated and shown in Figs. 9c and 9d.

The maximum allowed RT_{NDT} of the ring material, as shown in Figs. 9c and 9d, are 93 °C for the case based on CFD transient, and 106 °C, 118.7 °C and 139.3 °C for GRS-MIX and RELAP5 calculated transient. The corresponding maximum allowed RT_{NDT} of the welding material are 143.6 °C, 194.3 °C, 206 °C and 245.7 °C.

Compared to the maximum allowed RT_{NDT} determined from the deterministic method in Section 5, the maximum allowed RT_{NDT} from the probabilistic method is increased by more than 16 °C, since random variables are considered in the probabilistic analysis. This is because that in the deterministic analysis the most bounding value is used, while in the probabilistic analysis the scatter of random variables is considered and thus reduces the conservatism in the deterministic analysis. The use of most bounding variables excludes crack initiation whereas in the probabilistic analyses, probabilities for crack initiation are calculated.

7. Conclusions

Based on this study, the following conclusions are drawn:

1. A comprehensive framework coupling reactor system, fluid dynamics, fracture mechanics and probabilistic analyses for the integrity analysis of RPVs subjected to PTS loadings is proposed. Probabilistic study of the RPV considering the non-uniform cooling effect is performed. A series of transients, initiated by a break in the hot leg, is simulated with RELAP5, GRS-MIX and CFD with and without considering non-uniform cooling effect. Stress intensity factors are evaluated by FEM, XFEM and FAVOR codes.
2. The comparison of stress intensities calculated based on the different thermal-hydraulic tools (RELAP5, GRS-MIX and CFD) showed large differences due to the differences in thermal hydraulic results. Peak K_I of the cracks inside the plume increases about 30% compared with that outside. K_I based on CFD input is the highest, followed by that based on GRS-MIX and RELAP5. Considering the non-uniform

plume cooling effects increases the total failure frequency by more than one order of magnitude. In order to be more realistic and not to be non-conservative, 3D CFD may be required for the safety analysis of the RPV.

3. Considering non-uniform cooling effect increased the crack tip constraint due to the increase of the stress in both axial and circumferential directions. The T-stress is influenced by loading, geometry and crack size. The cooling plume also has a significant influence on T-stress distributions.
4. In the deterministic analysis, according to the maximum criteria, the maximum allowed RT_{NDT} is 56.9 °C, for the crack in the nozzle region based on CFD transient, and 90.2 °C, 115.7 °C and 136.2 °C for the cracks in the ring region based on the CFD, GRS-MIX and RELAP5 calculated transient. These values are 36 °C, 68.5 °C, 81 °C and 104 °C according to the tangent criteria. Maximum allowed RT_{NDT} values are used to limit the lifetime of the reactor pressure vessel.
5. The safety margin is increased by more than 16 °C if a probabilistic method is applied. The ring made from base material is more critical than the welding material of the vessel. According to the probabilistic method, the maximum allowed RT_{NDT} values of the ring material are 93 °C, 118.7 °C and 139.3 °C for the case based on CFD transient, GRS-MIX and RELAP5 calculated transient, respectively. The corresponding maximum allowed RT_{NDT} values of the welding material are 143.6 °C, 206 °C and 245.7 °C.

Acknowledgements

The authors acknowledge the financial support of the PISA Project provided by the Swiss Federal Nuclear Safety Inspectorate (ENSI) (DIS-Vertrag Nr. H-100668). We are also thankful for providing the code GRS-MIX by the Gesellschaft für Anlagen- und Reaktorsicherheit GmbH (GRS).

References

1. Qian, G. (2014) Gonzalez-Albuixech VF, Niffenegger M. In-plane and out-of-plane constraint effects under pressurized thermal shocks. *Int. J. Solids. Struct.*, **6**, 1311-1321.
2. Qian, G., and Niffenegger, M. (2013) Integrity analysis of a reactor pressure vessel subjected to pressurized thermal shocks by considering constraint effect. *Eng. Fract. Mech.*, **112-113**, 14-25.
3. International Atomic Energy Agency. (2010) Pressurized Thermal Shock in Nuclear Power Plants: Good Practices for Assessment. *IAEA - TECDOC - 1627*. Austria: IAEA.
4. Qian, X.D., Jr., R.H., Yin, S.J., and Bass. R. (2008) Cleavage fracture modeling of pressure vessels under transient thermo-mechanical loading. *Eng. Fract. Mech.*; **75**, 4167-89.
5. Sun, X., Chai, G., and Bao, Y. (2017) Elastic and elastoplastic fracture analysis of a reactor pressure vessel

- 1
2
3
4
5
6
7
8
9 under pressurized thermal shock loading. *Eur. J. Mech. A-Solid.*, **66**, 69-78.
- 10
11 6. Dickson, T.L., Williams, P.T., and Yin, S. (2007) Fracture analysis of vessels-Oak Ridge FAVOR, v 06.1:
12 computer code: user's guide. *NUREG-ORNL/TM-2007/031*.
- 13
14 7. Bass, B.R., Pugh, C.E., Sievers, J., and Schulz, H. (1999) International comparative assessment study of
15 pressurized thermal shock in reactor pressure vessel. *NUREG/CR-6651*.
- 16
17 8. U.S. Nuclear Regulatory Commission (2010) Section 50.61a of the Code of Federal Regulations, "Alternate
18 Fracture Toughness Requirements for Protection Against Pressurized Thermal Shock Events," 10 CFR
19 50.61a. US NRC, Washington.
- 20
21 9. U.S. Nuclear Regulatory Commission (2007) Technical Basis for Revision of the Pressurized Thermal
22 Shock (PTS) Screening Limit in the PTS Rule (10 CFR 50.61). *NUREG-1806*, Vol. 1, US NRC,
23 Washington.
- 24
25 10. Moinereau, D., and Bezdikian, G. (2008) Structural Margin Improvements in Age-embrittled RPVs with
26 Load History Effects (SMILE). *Contract FIKS-CT2001-00131*.
- 27
28 11. Simonen, F.A., Doctor, S.R., Schuster, G.J., and Heasler, P.G. (2004) A generalized procedure for
29 generating flaw-related inputs for the FAVOR code. *NUREG/CR-6817*.
- 30
31 12. Taylor, N., Nilsson, K., Minnebo, P., Bass, B., McAfee, W., Williams, P., Swan, D., and Siegele, D. (2005)
32 An Investigation of the Transferability of Master Curve Technology to Shallow Flaws in Reactor Pressure
33 Vessel Applications. *NESC IV (EUR 21846 EN)*.
- 34
35 13. Keim, E., Schmidt, C., Schöpfer, A., and Hertlein, R. (2001) Life management of reactor pressure vessels
36 under pressurized thermal shock loading: deterministic procedure and application to Western and Eastern
37 type of reactors. *Int. J. Pres. Vess. Piping*, **78**, 85-98.
- 38
39 14. Marie, S., Menager, Y., and Chapuliot, S. (2005) Stress intensity factors for underclad and through clad
40 defects in a reactor pressure vessel submitted to a pressurized thermal shock. *Int. J. Pres. Vess. Piping*, **82**,
41 746-760.
- 42
43 15. Yu, M., Luo, Z., and Chao, Y. J. (2015) Correlations between Charpy V-notch impact energy and fracture
44 toughness of nuclear reactor pressure vessel (RPV) steels. *Eng. Fract. Mech.*, **147**, 187-202
- 45
46 16. Chou, H.W., and Huang, C.C. (2014) Effects of fracture toughness curves of ASME Section XI - Appendix
47 G on a reactor pressure vessel under pressure-temperature limit operation. *Nucl. Eng. Des.*; **280**, 404-412.
- 48
49 17. Chou, H.W., and Huang, C.C. (2014) Structural reliability evaluation on the pressurized water reactor
50 pressure vessel under pressurized thermal shock events. *Proceedings of the ASME 2014 Pressure Vessels &
51 Piping Division Conference, PVP2014-28350, Anaheim, California, USA, 2014*.

- 1
2
3
4
5
6
7
8
9
10 18. Qian, G., Niffenegger, M. (2013) Procedures, methods and computer codes for probabilistic assessment of
11 reactor pressure vessels subjected to pressurized thermal shocks. *Nucl. Eng. Des.*; **258**, 35-50.
- 12 19. Qian, G., and Niffenegger, M. (2014) Deterministic and probabilistic analysis of a reactor pressure vessel
13 subjected to pressurized thermal shocks. *Nucl. Eng. Des.*; **273**, 381-95.
- 14 20. Sun, X., Chai, G., and Bao, Y. (2017) Nonlinear numerical study of crack initiation and propagation in a
15 reactor pressure vessel under pressurized thermal shock using XFEM. *Fatigue Fract. Eng. Mater. Struct.*, 1–
16 13. <https://doi.org/10.1111/ffe.12689>
- 17 21. González-Albuixech, V.F., Qian, G., Sharabi, M., Niffenegger, M., Niceno, B., and Lafferty, N. (2015)
18 Comparison of PTS Analyses of RPVs based on 3D-CFD and RELAP5. *Nucl. Eng. Des.*; **291**, 168-78.
- 19 22. Qian, G., González-Albuixech, V.F., Niffenegger, M., and Sharabi, M. (2016) Probabilistic PTS analysis for
20 a reactor pressure vessel considering plume cooling effect. *ASME J. Press. Vess. Tech.*, **138**, 041204-1-
21 041204-8.
- 22 23. SCIENTECH Inc. (1999) RELAP5/Mod3 Code Manual, vol. I: Code Structure, System Models and
23 Solution Methods. The Thermal Hydraulics Group, Idaho.
- 24 24. Mahaffys, J., Chung, B., Dubois, F., et al. (2007) Best Practice Guidelines for the Use of CFD in Nuclear
25 Reactors Safety Applications. *NEA/CSNI/R*.
- 26 25. Damerell, P.S., Simonis, J.W. (1992) 2D/3D Program Work Summary Report. *NUREG/IA-0126*.
- 27 26. Sonnenburg, H.G. (1997) Phänomenologische Versuchsauswertung des Versuchs UPTF-TRAM C1
28 Thermisches Mischen im Kaltstrang. *GRS-A-2434*.
- 29 27 Chen, .C.J., and Chen, C.H. (1979) On Prediction and Unified Correlation for Decay of Vertical Bouyant
30 Jets. *Trans. ASME*, Vol. **101**, 532-537.
- 31 27-28. [Sharabi, M., Gonzalez-Albuixech, V.F., Lafferty, N., Niceno, B. and Niffenegger, M. \(2016\)](#)
32 [Computational Fluid Dynamics Study of Pressurized Thermal Shock in the Reactor Pressure Vessel. *Nucl.*](#)
33 [Eng. Des.](#); **297**, 111-122.
- 34 28-29. Hibbitt, Karlsson, Sorensen (2017). *Abaqus 6.14.3 Manual*.
- 35 29-30. Bückner, H. (1970) A novel principle for the computation of stress intensity factors. *ZAMM* **50**, 529-546.
- 36 30-31. Moës, N., Dolbow, J., and Belytschko, T. (1999) A finite element method for crack growth without
37 remeshing. *Int. J. Num. Methods Eng.*, **46**,131–150.
- 38 31-32. ASME code (1995). ASME boiler and pressure vessel code, section III, nuclear power plant
39 components. New York.
- 40 32-33. ASME code (1997). ASTM-E1921-02. Test method for determination of reference temperature, T_0 , for
41
42
43
44
45
46
47
48
49
50

ferritic steels in the transition range. New York.

~~33-34~~ Wang, X. (2003) Elastic T-stress solutions for semi-elliptical surface cracks in finite thickness plates. *Eng. Fract. Mech.*; **70**, 731-756.

~~34-35~~ Zhu, X.K., and Joyce, J.A. (2012) Review of fracture toughness (G, K, J, CTOD, CTOA) testing and standardization. *Eng. Fract. Mech.*; **85**, 1-46.

~~35-36~~ Hohe, J., Brand, M., and Siegele, D. (2010) Behaviour of sub-clad and through-clad cracks under consideration of the residual stress field. *Eng. Fract. Mech.*; **77**, 217-228.

~~36-37~~ Chao, Y.J., Yang, S., and Sutton, M.A. (1994) On the fracture of solids characterized by one or two parameters: Theory and practice. *J. Mech. Phys. Solids*, **42**, 629-647.

Review Copy

1
2
3
4
5
6
7
8
9
10 **List of Table/Figure Captions:**
11
12
13

14 Table 1 Conditional failure probabilities and total failure frequency, calculated with FAVOR and based on
15 RELAP5, GRS-MIX and CFD calculated transients.

17 Fig. 1a Physical model for the integrity analysis of a reactor pressure vessel. Fig. 1b Flowchart in the
18 probabilistic fracture mechanics analysis. Fig. 1c Demonstration of applied numerical methods in the safety
19 assessment of a RPV.
20

21 Fig. 2a Coolant temperature in the downcomer at core height for various hot leg break sizes (cm^2) calculated
22 with RELAP5. Fig. 4b Reactor coolant system pressure for various hot leg break sizes (cm^2) calculated with
23 RELAP5. Fig. 4c HTC in the downcomer for various hot leg break sizes (cm^2) calculated with RELAP5. Fig. 4d
24 Coolant temperature in the downcomer at the core height for various hot leg break sizes (cm^2) calculated with
25 GRS-MIX. Fig. 2e Heat transfer coefficient history of the studied transients calculated with GRS-MIX.
26

27 Fig. 3a Structured mesh of the RPV for CFD. Fig. 3b Partial view of the mesh. Fig. 3c Temperature distribution
28 at the inner RPV wall for the SBLOCA calculated with CFD. Fig. 3d Temperature distribution at the inner RPV
29 wall for the MBLOCA calculated with CFD. Fig. 3e von-Mises stress distribution (unit: Pa) at the inner RPV
30 wall for the SBLOCA calculated with CFD. Fig. 3f von-Mises stress distribution (unit: Pa) at the inner RPV
31 wall for the MBLOCA calculated with CFD. Fig. 3g von-Mises stress distribution (unit: Pa) at the inner RPV
32 wall for the MBLOCA calculated with CFD.
33

34 Fig. 4a Overview of the mesh and crack details for axial crack using FEM. Fig. 4b Overview of the mesh and
35 crack details for axial crack using XFEM. The overlap of the elliptical surface and the cylinder defines the
36 crack. Fig. 4c Overview of the mesh and crack details for cracks in inlet nozzle using XFEM. The overlap of the
37 elliptical surface and the cylinder defines the crack.
38

39 Fig. 5a Comparison of KI calculated by FAVOR, FEM and XFEM for surface crack $2c/a=6$, $a=17$ mm and the
40 MBLOCA. Fig. 5b Inner vessel wall temperature for MBLOCA, with and without considering non-uniform
41 cooling. Fig. 5c Inner vessel wall temperature for SBLOCA, with and without considering non-uniform cooling.
42 Fig. 6a Comparison of K_I values by considering non-uniform cooling, MBLOCA. Fig. 6b Comparison of K_I
43 values of the RPV by considering non-uniform cooling, SBLOCA. Fig. 6c Comparison of T-stress by
44 considering non-uniform cooling, MBLOCA. Fig. 6d Comparison of T-stress by considering non-uniform
45 cooling, SBLOCA.
46
47
48

49 Fig. 7a Crack distributions of the surface and embedded cracks assumed in the probabilistic study. Fig. 7b
50

1
2
3
4
5
6
7
8
9
10
11
12
13
14
15
16
17
18
19
20
21
22
23
24
25
26
27
28
29
30
31
32
33
34
35
36
37
38
39
40
41
42
43
44
45
46
47
48
49
50
51
52
53
54
55
56
57
58
59
60

Probability for different transients based on RELAP5, GRS-MIX and CFD calculated transients.
Fig. 8 Maximum and tangent criteria to determine allowed RT_{NDT} for the surface crack postulated in the nozzle and ring.
Fig. 9a Proposal of PTS screening limit based on probabilistic estimate of through-wall cracking frequency (TWCF) acceptance criterion [8, 9]. Fig. 9b Fittings between through-wall cracking frequency and the maximum RT_{NDT} for welding and ring materials. Fig. 9c Comparison of maximum RT_{NDT} from probabilistic method with that from the maximum criteria of the deterministic method for ring and welding materials Fig. 9d Comparison of maximum RT_{NDT} from probabilistic method with that from the tangent criteria of the deterministic method for ring and welding materials.

Review Copy

	3 cm ² (SBLOCA)	70 cm ² (MBLOCA)	450 cm ² (LBLOCA)	Total failure frequency
Transient occurrence frequency	4.62×10^{-3}	4.52×10^{-4}	3.30×10^{-6}	
Conditional failure probability or total failure frequency (RELAP5)	5.49×10^{-7}	1.00×10^{-13}	1.00×10^{-13}	2.54×10^{-9}
Conditional failure probability or total failure frequency (GRS-MIX)	6.36×10^{-6}	9.51×10^{-7}	1.00×10^{-13}	2.98×10^{-8}
Conditional failure probability or total failure frequency (CFD)	1.00×10^{-13}	4.57×10^{-4}		2.07×10^{-7}

Table 1 Conditional failure probabilities and total failure frequency, calculated with FAVOR and based on RELAP5, GRS-MIX and CFD calculated transients.

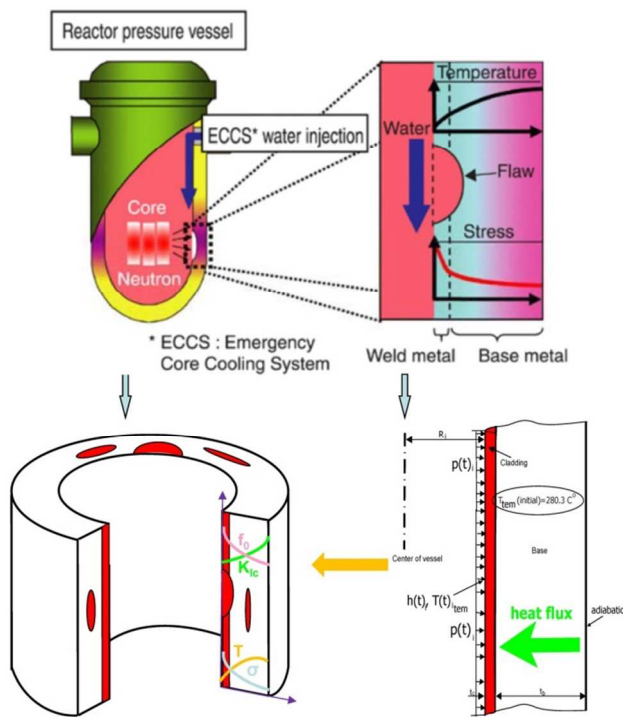


Fig. 1a Physical model for the integrity analysis of a reactor pressure vessel.

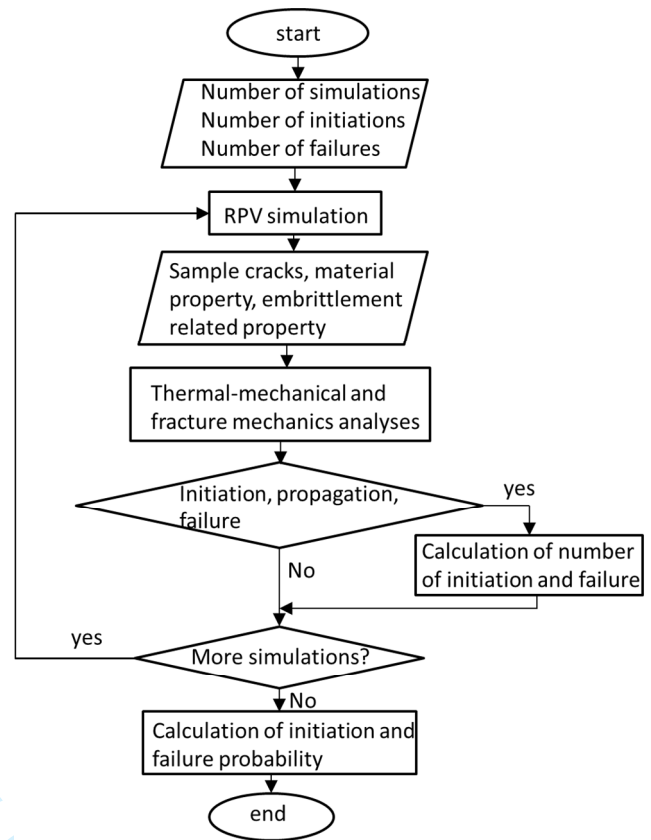


Fig. 1b Flowchart in the probabilistic fracture mechanics analysis.

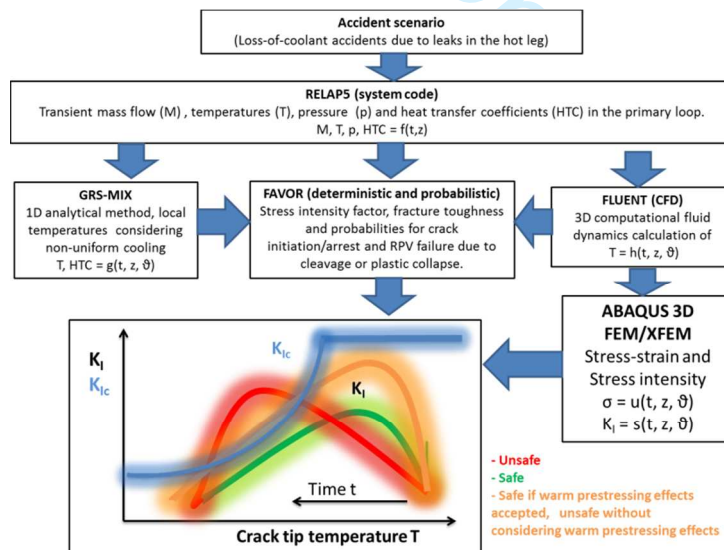


Fig. 1c Demonstration of applied numerical methods in the safety assessment of a RPV.

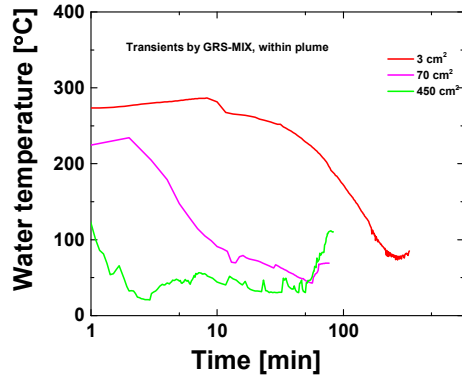
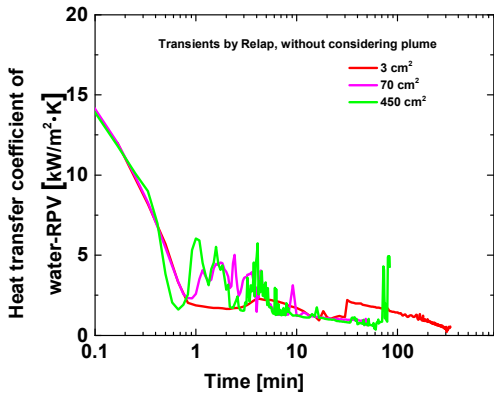


Fig. 2c HTC in the downcomer for various hot leg break sizes (cm^2) calculated with RELAP5.

Fig. 2d Coolant temperature in the downcomer at the core height for various hot leg break sizes (cm^2) calculated with GRS-MIX.

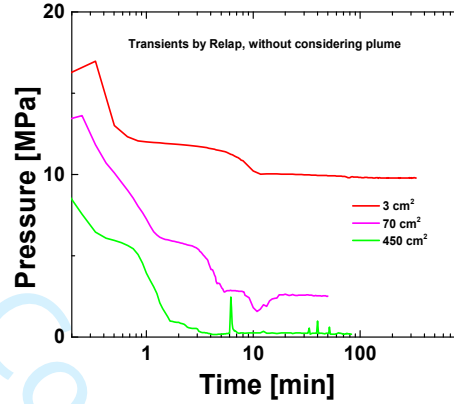
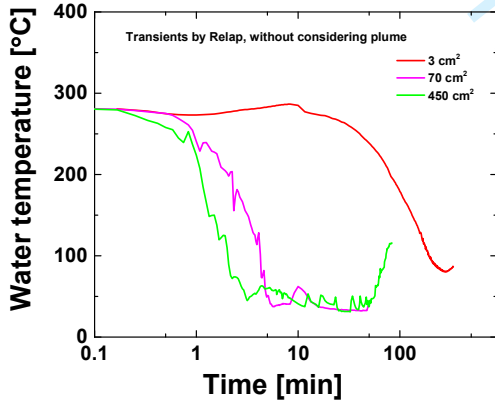


Fig. 2a Coolant temperature in the downcomer at core height for various hot leg break sizes (cm^2) calculated with RELAP5.

Fig. 2b Reactor coolant system pressure for various hot leg break sizes (cm^2) calculated with RELAP5.

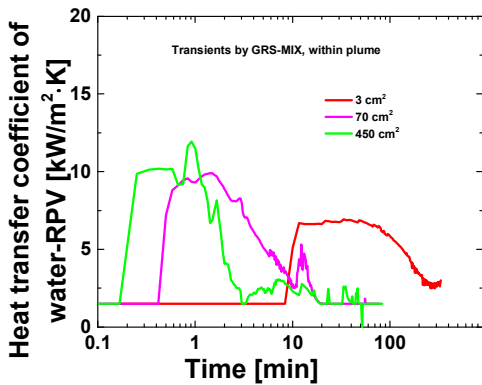


Fig. 2e Heat transfer coefficient history of the studied transients calculated with GRS-MIX.

1
2
3
4
5
6
7
8
9
10
11
12
13
14
15
16
17
18
19
20
21
22
23
24
25
26
27
28
29
30
31
32
33
34
35
36
37
38
39
40
41
42
43
44
45
46
47
48
49
50
51
52
53
54
55
56
57
58
59
60

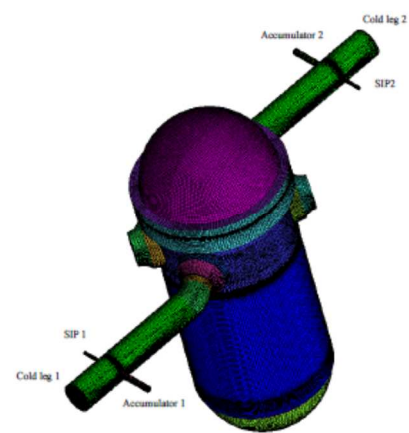


Fig. 3a Structured mesh of the RPV for CFD.

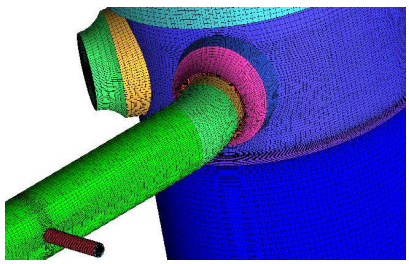


Fig. 3b Partial view of the mesh.

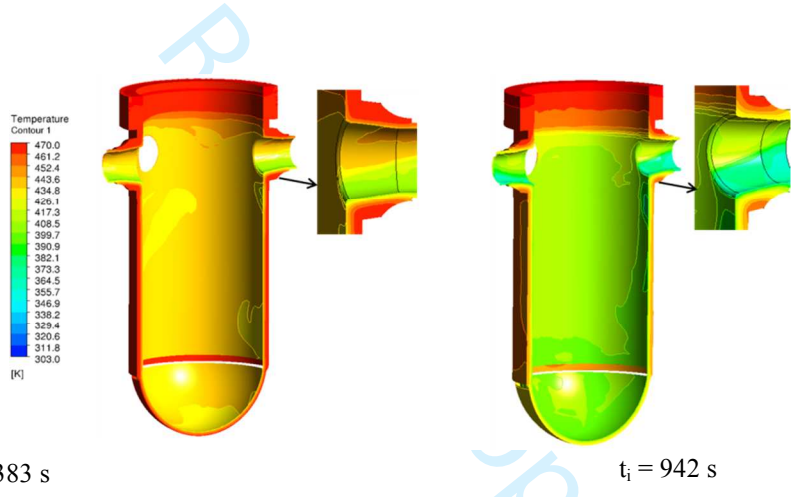


Fig. 3c Temperature distribution at the inner RPV wall for the SBLOCA calculated with CFD.

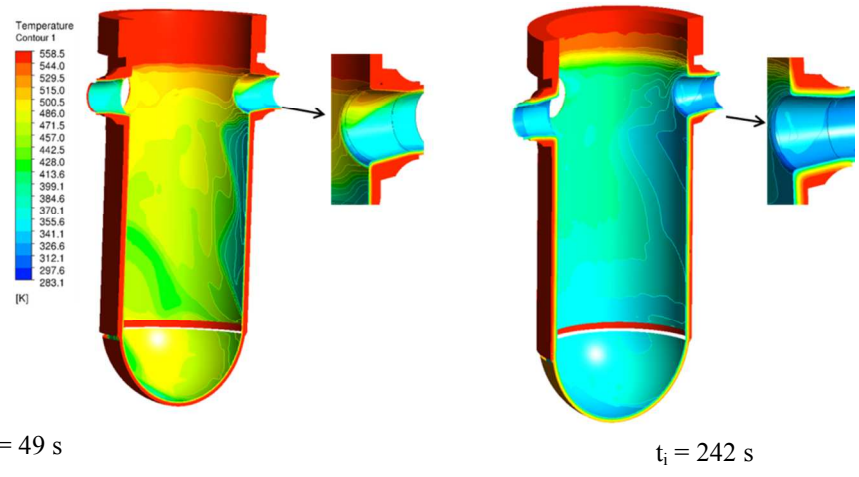


Fig. 3d Temperature distribution at the inner RPV wall for the MBLOCA calculated with CFD.

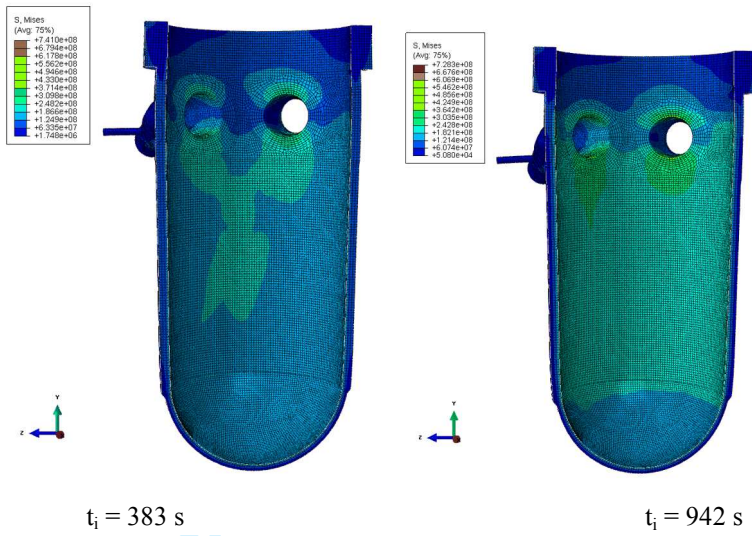


Fig. 3e von-Mises stress distribution (unit: Pa) at the inner RPV wall for the SBLOCA calculated with CFD.

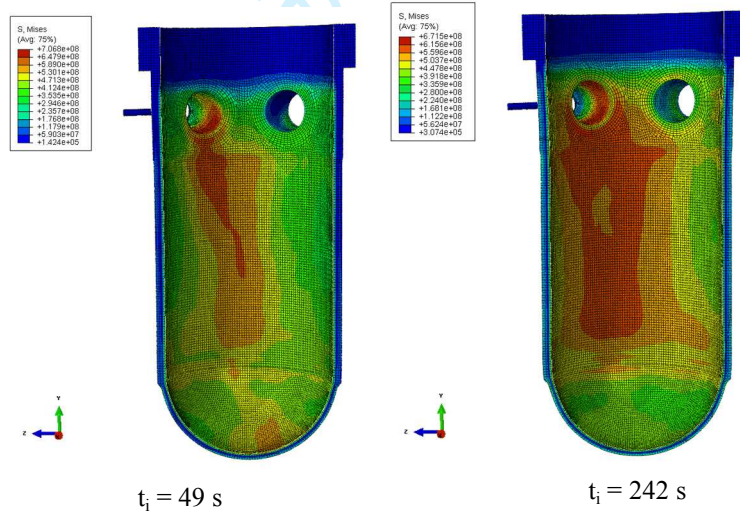


Fig. 3f von-Mises stress distribution (unit: Pa) at the inner RPV wall for the MBLOCA calculated with CFD.

1
2
3
4
5
6
7
8
9
10
11
12
13
14
15
16
17
18
19
20
21
22
23
24
25
26
27
28
29
30
31
32
33
34
35
36
37
38
39
40
41
42
43
44
45
46
47
48
49
50
51
52
53
54
55
56
57
58
59
60

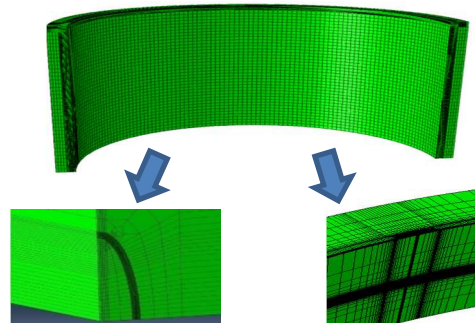


Fig. 4a Overview of the mesh and crack details for axial crack using FEM.

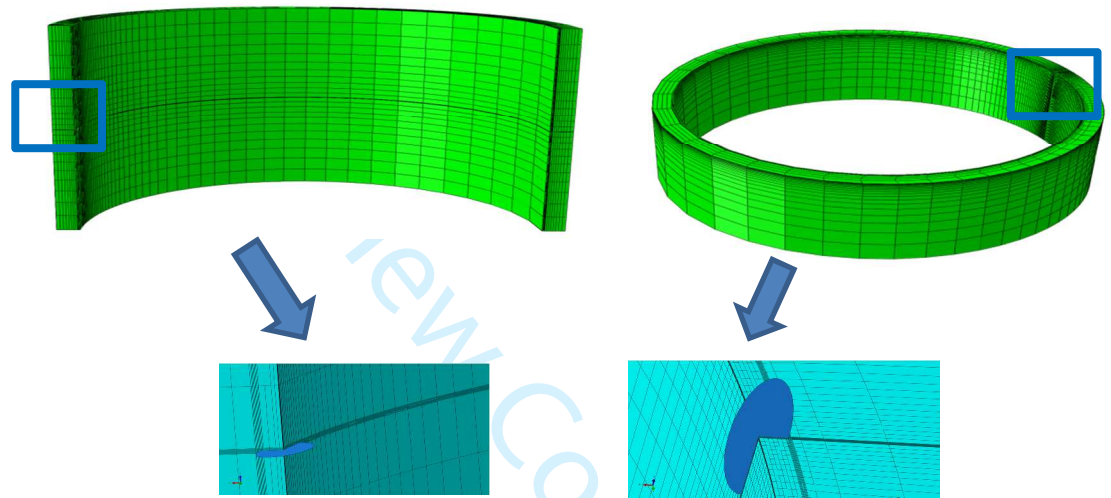


Fig. 4b Overview of the mesh and crack details for axial crack using XFEM. The overlap of the elliptical surface and the cylinder defines the crack.

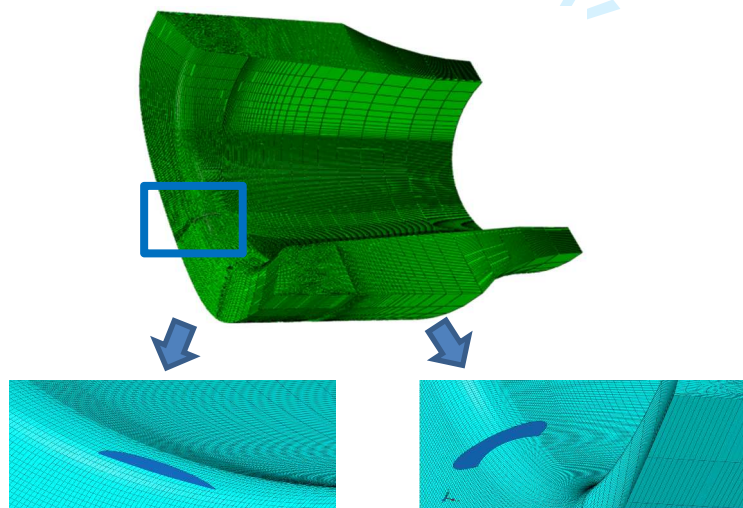


Fig. 4c Overview of the mesh and crack details for cracks in inlet nozzle using XFEM. The overlap of the elliptical surface and the cylinder defines the crack.

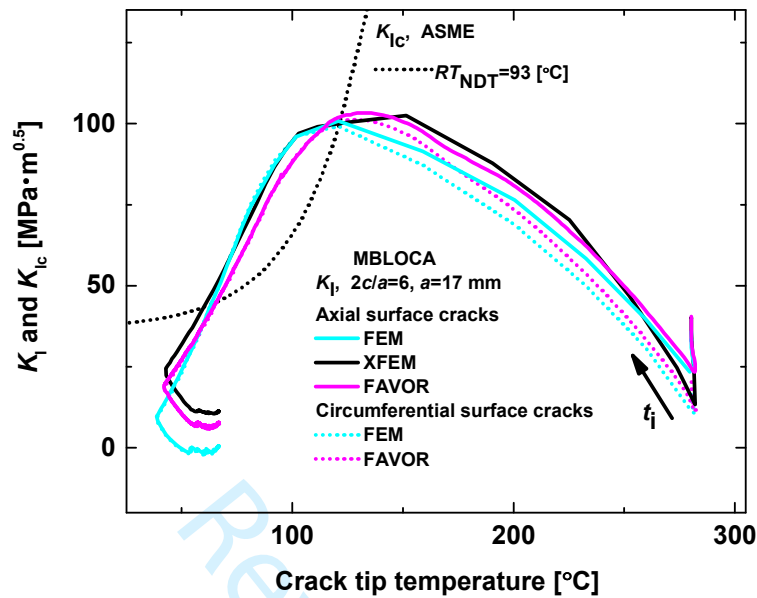


Fig. 5a Comparison of K_I calculated by FAVOR, FEM and XFEM for surface crack $2c/a=6$, $a=17$ mm and the MBLOCA.

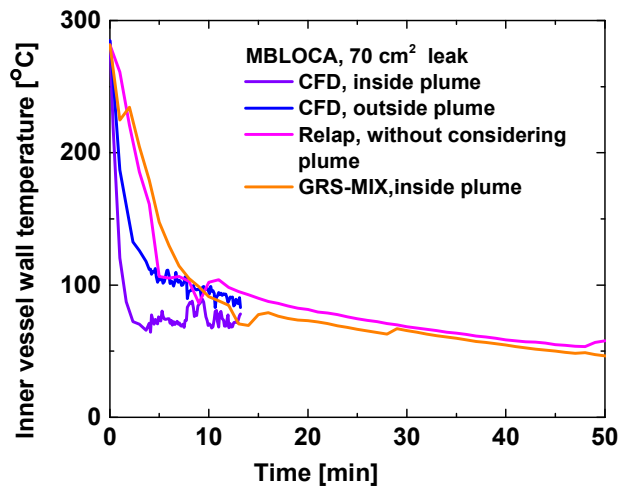


Fig. 5b Inner vessel wall temperature for MBLOCA, with and without considering non-uniform cooling.

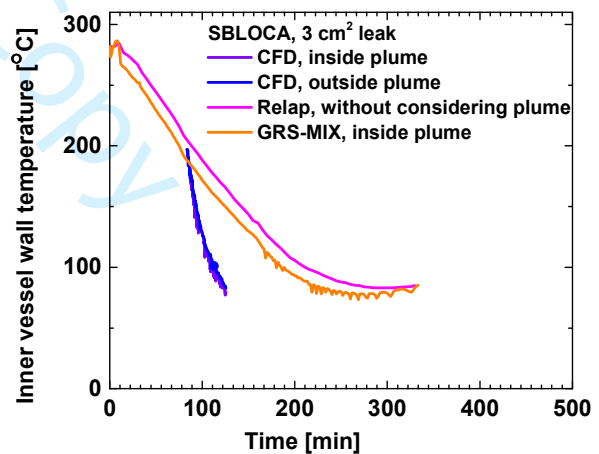


Fig. 5c Inner vessel wall temperature for SBLOCA, with and without considering non-uniform cooling.

1
2
3
4
5
6
7
8
9
10
11
12
13
14
15
16
17
18
19
20
21
22
23
24
25
26
27
28
29
30
31
32
33
34
35
36
37
38
39
40
41
42
43
44
45
46
47
48
49
50
51
52
53
54
55
56
57
58
59
60

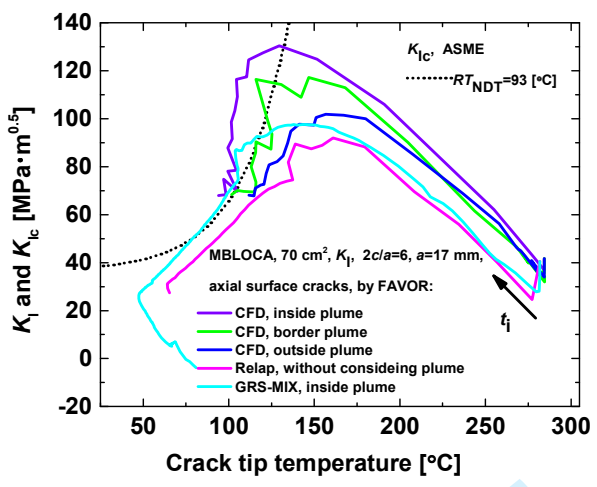


Fig. 6a Comparison of K_I values by considering non-uniform cooling, MBLOCA.

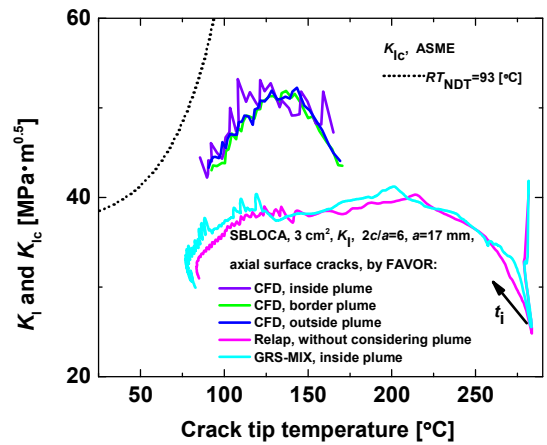


Fig. 6b Comparison of K_I values of the RPV by considering non-uniform cooling, SBLOCA

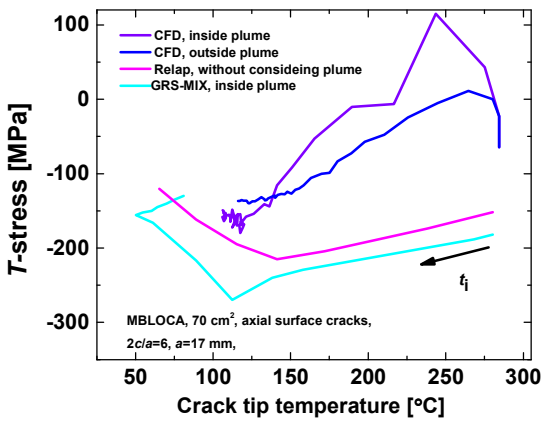


Fig. 6c Comparison of T-stress by considering non-uniform cooling, MBLOCA.

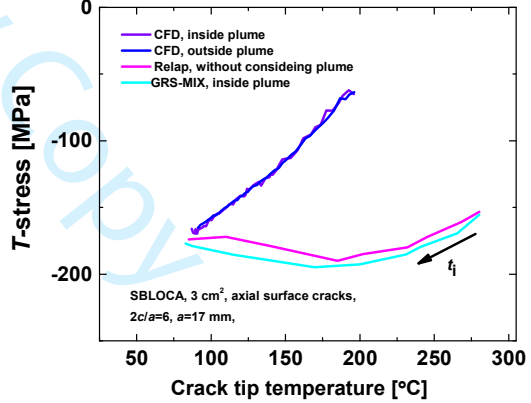


Fig. 6d Comparison of T-stress by considering non-uniform cooling, SBLOCA.

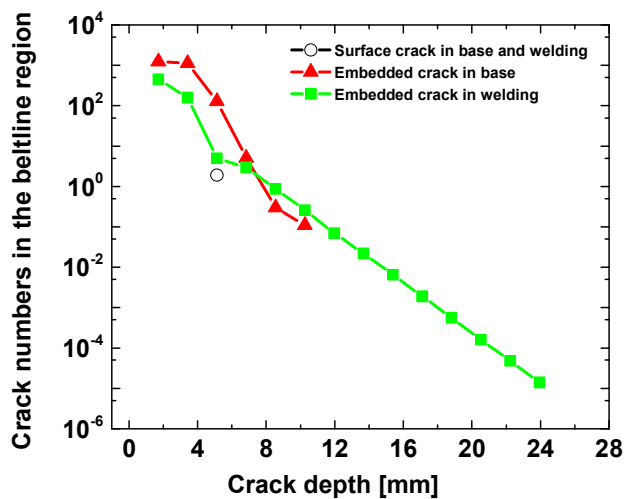


Fig. 7a Crack distributions of the surface and embedded cracks assumed in the probabilistic study.

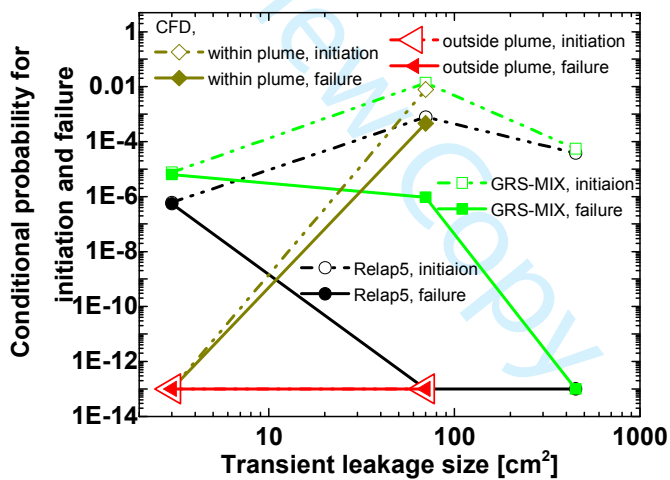


Fig. 7b Probability for different transients based on RELAP5, GRS-MIX and CFD calculated transients.

1
2
3
4
5
6
7
8
9
10
11
12
13
14
15
16
17
18
19
20
21
22
23
24
25
26
27
28
29
30
31
32
33
34
35
36
37
38
39
40
41
42
43
44
45
46
47
48
49
50
51
52
53
54
55
56
57
58
59
60

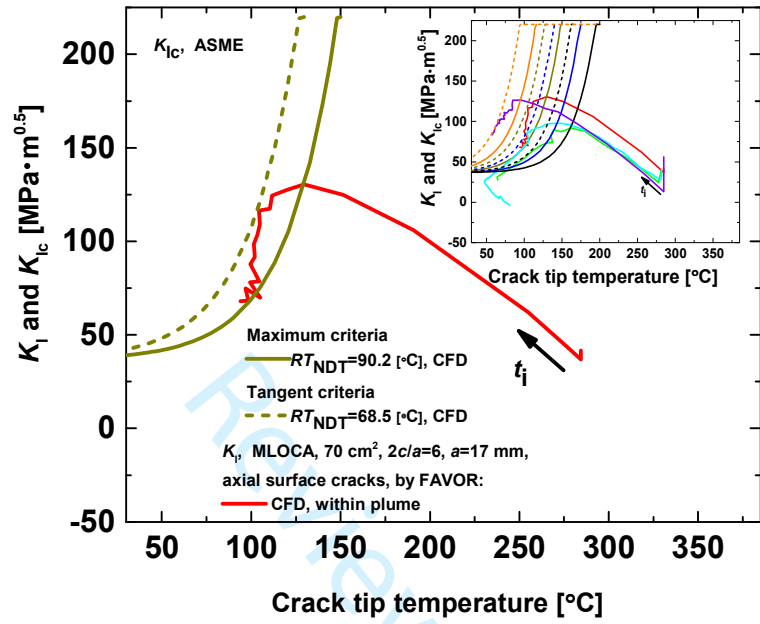


Fig. 8 Maximum and tangent criteria to determine allowed RT_{NDT} for the surface crack postulated in the nozzle and ring

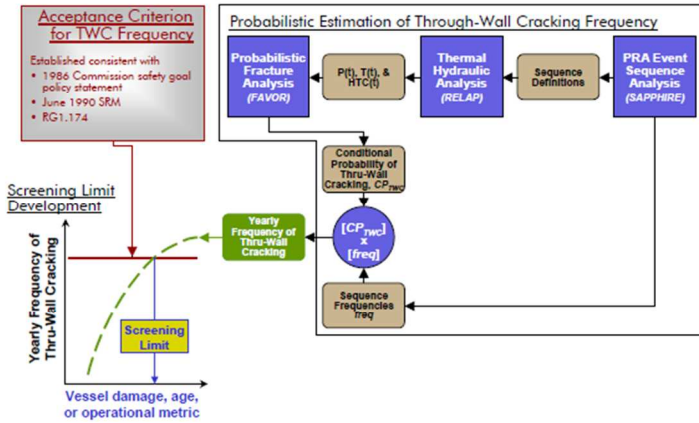


Fig.9a Proposal of PTS screening limit based on probabilistic estimate of through-wall cracking frequency (TWCF) acceptance criterion [8, 9].

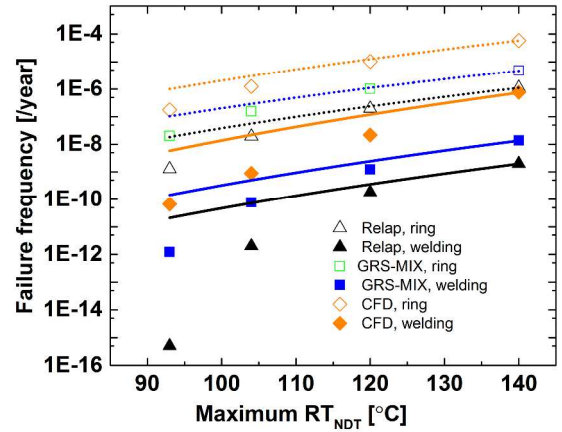


Fig.9b Fittings between through-wall cracking frequency and the maximum RT_{NDT} for welding and ring materials.

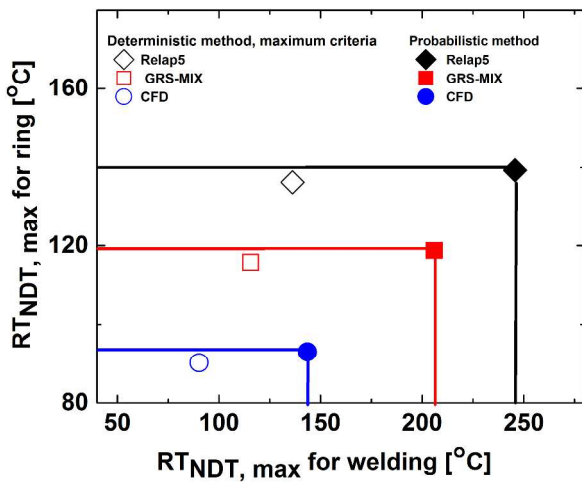


Fig. 9c Comparison of maximum RT_{NDT} from probabilistic method with that from the maximum criteria of the deterministic method for ring and welding materials.

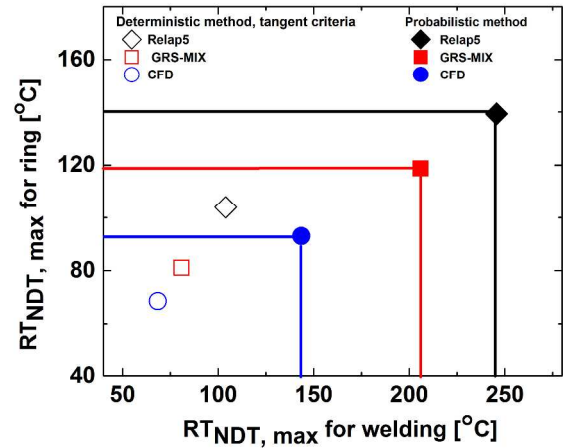


Fig. 9d Comparison of maximum RT_{NDT} from probabilistic method with that from the tangent criteria of the deterministic method for ring and welding materials.



Laboratory for Nuclear Materials
CH-5232 Villigen PSI
Switzerland

Telephone 0041 56 /310 28 65

E-mail guian.qian@psi.ch

Villigen, 20. 01. 2018

Response to Reviewers' Comments

Re: FFEMS-7296: Fatigue & Fracture of Engineering Materials & Structures

Title: Effect of non-uniform reactor cooling on fracture and constraint of a reactor pressure vessel

Dear Prof. Hong,

Thank you very much for sending us the reviewers' comments for our above mentioned paper. We appreciate very much the insightful comments raised by the reviewers, which allowed us to improve the quality of the paper. We have carefully revised this manuscript according to the reviewers' comments. The modifications are listed point by point below:

[Reviewer: 1]

Overall, the paper presents a sound approach, and is recommended for publication with revisions. There are a few areas where more explanation of the methods used is needed:

1) More explanation of GRS-MIX is needed. It is obvious that RELAP5 and 3D CFD are very different approaches for computing the thermal environment in the coolant, but it is not clear from the text what is unique about the GRS-MIX approach, and how it is distinguished from the other approaches. A short paragraph summarizing the distinguishing features of that model and the motivation for using it would go a long way.

Response: We acknowledge the useful comments recommended by the reviewer which help to clarify our results. According to the comments, an additional explanation is added to show the motivation of using GRS-MIX and its distinguishing feature, as

RELAP5 and other similar system codes can predict integral behavior of the reactor during transients and give predictions of relevant variables fairly well without the need of high computational resources. Nevertheless, these methods fail to predict local effects and three-dimensional phenomena such as those taking place during PTS. It is therefore needed to adopt other methods that are more accurate and also computationally efficient. Within this framework, GRS-MIX is used which is a software developed by GRS (Gesellschaft für Anlagen- und Reaktorsicherheit). The code has a number of implemented engineering correlations and the relevant correlations can be used based on the estimated flow regime. The output of the code gives the temperatures and heat transfer coefficients at the prescribed positions downstream in the downcomer.

2) In section 3, explain why FAVOR is used with the RELAP5 and GRS-MIX outputs, whereas XFEM is used for the 3D CFD models.

Response: According to the comments, the following sentences are now added in the text to clarify the reasons:

RELAP5 and GRS-MIX outputs are one-dimensional, meaning that the calculated coolant temperature, pressure and heat transfer coefficient are uniform in the inner vessel wall and they only vary with the transient time. However, the output with 3D CFD models is non-uniform in the vessel wall. In the FAVOR code, it is assumed that the coolant is uniform in the inner vessel wall and FAVOR is thus not able to capture the non-uniform cooling effect. 3D XFEM is resorted to analyze the non-uniform cooling effect on K_I .

1
2
3
4 3) In Section 2.3, you talk about the results not changing much with different meshes. More detail is
5 needed. Were those meshes coarser or finer than the one chosen for the final analyses?
6

7 **Response:** The final analyses were conducted using the finer mesh. Further information is added to
8 describe details about the mesh sensitivity, as:
9

10 In order to study mesh sensitivity of the results, two meshes were constructed using fully structured
11 mesh topology with 3.3 and 5.1 million nodes. Special attention was taken to have more refinement
12 in locations of the plumes and cold legs where injection of cold water is expected. No significant
13 differences of the plume behavior or temperature distributions were noticed for the case of higher
14 mass flow rate injection of cold water. All the simulations in the current study were conducted
15 making use of the finer mesh shown in Figs. 3a and b. Further details about mesh strategy adopted
16 in the present study can be found in [28].
17
18

19
20 [28] Sharabi, M., Gonzalez-Albuixech, V.F., Lafferty, N., Niceno, B. and Niffenegger, M. (2016)
21 Computational Fluid Dynamics Study of Pressurized Thermal Shock in the Reactor Pressure Vessel.
22 *Nucl. Eng. Des.*; **297**, 111-122.
23
24

25
26 4) In section 3, more details are needed on the geometry of the crack used to compare FAVOR,
27 FEM and XFEM.
28

29 **Response:** An axial semi-elliptical crack, which has the depth of 17 mm and aspect ratio
30 (length/depth) of 6 is postulated in the deterministic analysis. The crack geometry is according to
31 German KTA rule, which is consistent with the two times nondestructive examination limit.
32
33

34 This is now included in the text.
35
36
37

38 5) In section 4.1.1, it is stated that the FAVOR code was modified to allow reading of temperature
39 distributions. That warrants more explanation. Since FAVOR typically computes the thermal and
40 mechanical response, I assume that means that it was modified to only compute the mechanical
41 response with a given prescribed through-wall temperature distribution. Is that the case?
42
43

44 Also, is this change only applicable for deterministic analyses, or is it also applicable for
45 probabilistic analyses?
46

47 **Response:** This change of FAVOR is applicable for both deterministic and probabilistic analyses.
48 FAVOR was modified to compute the mechanical response with a given prescribed through-wall
49 temperature distribution from the 3D CFD calculation. The given through-wall temperature is taken
50 from either within or outside of the plume in the 3D RPV model. Since FAVOR is a probabilistic
51 code, the modified FAVOR is also used to perform probabilistic fracture mechanics analysis with
52 the 3D CFD output.
53
54
55
56

1
2
3
4 According to the comments, the sentences are now added in the manuscript.
5
6
7

8 6) From reading through the text, it is not really clear how the probabilistic fracture mechanics
9 analysis is conducted. For the deterministic analyses, a small number of flaws are considered. In
10 section 4.2, it sounds like a large population of flaws is considered for the probabilistic analysis. It
11 is feasible that FAVOR could be used for the RELAP5 and GRS-MIX thermal models, but it isn't
12 clear how a population of flaws is considered for the 3D CFD case. Are detailed XFEM models run
13 of hundreds of flaws using ABAQUS? Are those results somehow fed into FAVOR, or is the
14 probabilistic analysis done using a separate code? More explanation is needed.
15
16

17 **Response:** For the deterministic analyses, only a fixed crack is considered. A large population of
18 cracks is considered for the probabilistic analysis. The distributions of cracks, density, depth, aspect
19 ratio are described in the manuscript. FAVOR is used for probabilistic fracture mechanics analysis
20 based on the output of RELAP5, GRS-MIX and 3D CFD calculations. The FAVOR code is
21 modified to compute the mechanical response and perform probabilistic analysis with a given
22 prescribed through-wall temperature distribution taken from 3D CFD analysis. The results from
23 XFEM models are used only in deterministic analysis to compare and validate the stress intensities.
24
25

26 According to the comments, the sentences are now added in the manuscript.
27
28
29
30

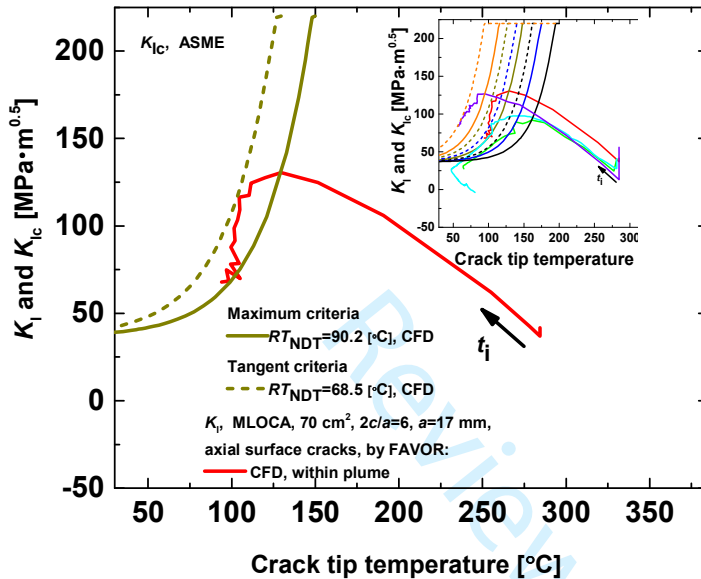
31 7) The maximum and tangent criteria for the deterministic method in section 5 could use a little
32 more explanation. Figure 8 is really busy because it has so many different cases. It would be good
33 to have a separate figure that just shows a single case to clearly illustrate these two criteria.
34
35

36
37 **Response:** According to the comments, the introduction of the maximum and tangent criteria is
38 explained in more detail, as
39

40
41 This is computed by shifting the K_{Ic} -temperature curve until it is intersected to their peak value if
42 warm prestressing (WPS)-effects are considered or tangent to the calculated K_I -temperature curve
43 of the transient under investigation. If the K_{Ic} -temperature curve is tangent to the K_I -temperature
44 curve, K_{Ic} is always higher than K_I during the whole transient and thus no crack initiation occurs.
45 WPS effect means that no crack initiation will occur if the material has been prestressed at a higher
46 temperature before reloaded above the K_{Ic} curve at a lower temperature. In the safety margin
47 analysis, the maximum criteria can be used if the WPS effect is considered. For the same K_I -
48 temperature curve, the maximum criteria predicts a larger safety margin and thus decreases the
49 conservatism of the results. According to both tangent and maximum criterion, the maximum
50 allowed RT_{NDT} of the irradiated RPV is determined. In this part, the maximum allowed RT_{NDT}
51
52
53
54
55
56

values according to maximum and tangent criteria for the axial surface crack with a depth of 17 mm and aspect ratio of 6 are evaluated, as shown in Fig. 8.

Figure 8 is redrawn to simplify the curves and show these two criteria, as



8) At the end of Section 6.2, it says 'since random variables are considered in the probabilistic analysis'. That's a pretty vague explanation. Either drop that part of that sentence, or explain in more detail why.

Response: According to the comments, a more detailed explanation is now added, as

“...the maximum allowed RT_{NDT} from the probabilistic method is increased by more than 16 °C. This is because that in the deterministic analysis the most bounding value is used, while in the probabilistic analysis the scatter of random variables is considered and thus reduces the conservatism in the deterministic analysis. The use of most bounding variables excludes crack initiation whereas in the probabilistic analyses, probabilities for crack initiation are calculated.”

In general, the paper could benefit from being edited for grammar, and the figures need to be improved to be publication quality. Here are some minor things I noted through the paper:

Page 2, Line 17: 'if probabilistic'->'if a probabilistic'

Page 2, Line 20: 'resulted'->'resulting'

1
2
3
4 Page 4, Line 10: 'resulted by the'->'the result of'

5
6 Page 4, Line 31: 'concerning'->'relevant' or 'uncertain'

7
8 Page 4, Line 36: 'failure results' -> 'cases resulting in failure'

9
10 Page 4, Line 44: 'temperatures'->'temperature'

11
12 Page 5, Line 10: 'parameters'->'parameter'

13
14 Page 6, Line 3: 'Transients'->'Transient'

15
16 Page 6, Line 24: 'Transients'->'Transient'

17
18 Page 6, Line 26: 'the break sizes that range' -> 'break sizes ranging'

19
20 Page 7, Line 3: 'but they are'->'are'

21
22 Page 7, Line 31: 'leg'->'legs'

23
24 Page 7, Line 35: 'A simulation time of 2500 s and 800 s were performed' -> 'Simulation times of
25 2500s and 800s were used'

26
27 Page 7, Line 38: 'inlet nozzles, especially' -> 'inlet nozzles. This is especially evident'

28
29 Page 8, Line 17: 'computation, i.e. the' -> 'computation: the'

30
31 Page 8, Line 20: 'implemented in FEM' -> 'implemented in the FEM (or XFEM) frameworks'

32
33 Page 8, Line 32: Explain variables b_i , Q , and a Page 8, Line 41: Explain M_m , σ_m , M_b ,
34 σ_b variables Page 8, Line 43: 'SIF'->'the SIF'

35
36 Page 8, Line 47: 'approach'->'approximation'

37
38 Page 8, Line 51: 'somehow'->'more'

39
40 Page 9, Line 10: 'with XFEM'->'represented using XFEM'

41
42 Page 9, Line 12: 'different databases'->'databases'

43
44 Page 9, Line 18: 'neutron'->'The neutron'

45
46 Page 10, Line 29: 'And'->'The'

47
48 Page 10, Line 38: 'variate'->'varies'

49
50 Page 11, Line 12: 'of ORNL database'->'fitted to data from an ORNL database'

51
52 Page 11, Line 23: 'crack'->'cracks'

1
2
3
4 Page 11, Line 32: 'output is higher'->'output are higher'

5
6 Page 11, Line 47: 'This indicates that' -> 'This is computed by shifting the KIC-temperature curve'

7
8 Page 12, Line 13: 'means that may' -> 'means that these results may'

9
10 Page 14, Line 15: 'from probabilistic' -> 'from the probabilistic'

11
12 Page 14, Line 26: 'Probabilistic'->'A probabilistic'

13
14 Many figures have axis labels with extremely large fonts. Reduce the size to better match the other
15 text.

16
17 Figures 2b, 2c, 2d, and 2e have the text 'Other transients'. It's not clear what 'other' means.

18
19 Figure 9d has a legend entry for 'reference transient', but there's no explanation of what that is, and
20 it doesn't show up on the plot.

21
22 **Response:** We appreciate the editing corrections by the reviewer. The editing grammar is now
23 corrected, the figure label fonts and text are also modified according to the comments.

24
25
26
27
28 **[Reviewer: 2]**

29
30
31
32
33 Comments to the Author

34
35 This paper simulate the PTS transients with three different methods (RELAP5, GRS-MIX,CFG)
36 firstly, then stress intensity factor is calculated with FAVOR code, FEM and XFEM. Some of the
37 conclusions in this paper is not convincing. The output of RELAP5 are used as input for the GRS-
38 mix, CFD and structural and fracture mechanics calculations. It is not clear whether the differences
39 between stress intensities calculated based on RELAP5, GRS-MIX and CFD is due to the
40 differences in thermal hydraulic results or from the error transfer in step by step calculations from
41 different models.

42
43
44 **Response:** We acknowledge the critical and constructive comments which help to improve our
45 paper. According to the comments, the following sentences are now added in the text to clarify the
46 differences between stress intensities calculated based on different methods:

47
48
49 RELAP5, GRS-MIX and CFD are three codes that adopt completely different approaches to
50 simulate the heating and mixing process of the injected cold water. RELAP5 is a best estimate one-
51 dimensional coarse-grid simulation code that is not capable to take into consideration the plume
52 cooling or thermal stratification, though it can provide the boundary conditions for other methods
53 based on the integral analyses of the transient. On the other hand, GRS-MIX is based on a number
54
55
56

1
2
3
4 of engineering correlations developed from UPTF-TRAM experiments for pressurized water
5 reactors. Different flow regimes can be distinguished and heating of the injected water can be
6 determined at different downstream positions in the downcomer. Though, due to geometrics
7 differences of the adopted design in the present study and differences in conditions (e.g.,
8 asymmetric injections), there is uncertainty in its predictions. CFD instead consider the exact details
9 of geometry and boundary conditions. Best practice guidelines were followed for meshing and
10 model selections.
11
12

13 From the above, the authors believe that the differences are greatly attributed to the different
14 approaches (and the validity of each method, especially for GRS-MIX when it is applied to different
15 geometry and different injection configurations) adopted in each code and CFD results are the most
16 realistic ones and there is no error transfer in steps of calculations. Though, CFD can be used only
17 for selected cases due to computational expenses, and a full analyses of PTS still need to rely on
18 other less detailed methods (such as engineering models or system codes) but also take into
19 consideration the uncertainty in the prediction as demonstrated in this paper.
20
21
22

23 A further statement is added to indicate the uncertainties of GRS-MIX, as:

24
25 Also, different thermal-hydraulic conditions like asymmetric cold water injections and injection of
26 cold water at two different locations in the same cold leg contribute to uncertainties regarding
27 validity of GRS-MIX correlations when applied to different problem configurations than those
28 developed for.
29
30
31
32
33
34
35
36
37
38
39
40
41
42
43
44
45
46
47
48
49
50
51
52
53
54
55
56

1
2
3
4
5
6
7
8
9
10
11
12
13
14
15
16
17
18
19
20
21
22
23
24
25
26
27
28
29
30
31
32
33
34
35
36
37
38
39
40
41
42
43
44
45
46
47
48
49
50
51
52
53
54
55
56
57
58
59
60

Yours sincerely,

Guian Qian, Markus Niffenegger, Medhat Sharabi, Nathan Lafferty

Review Copy

